An (EM)CCD Simulator in MATLAB

Nicholas Jones (njones31@vt.edu)

Graduate Research Assistant

VT National Security Institute, Mission Systems Division

Background

- Technology development program focused on answering heliophysics science questions
  - Funded through NASA ROSES Heliophysics Technology and Instrument Development for Science (H-TIDeS) program
  - PI: Dr. Leon Harding
- Developing instrument to measure nitric oxide in the polar night
  - Key constituent of the upper atmosphere
  - Involved in coupling of the Sun-Earth system
- Build on the results of sounding rocket flights as part of the PolarNOx program led by Co-PI Dr. Bailey
- NASA JPL Co-Is will be providing the camera electronics for the instrument

Program Timeline

Year 1

- Instrument design initiated
- Long lead-time procurement and manufacturing processes started
- Device optimization with commercial EMCCD camera system

Year 2

- Development of EMCCD camera electronics by JPL
- Camera system characterization by VT
- Environmental testing of camera system

Year 3

- Radiation testing
- Instrument characterization and testing

Camera system matured to TRL-6

Science

- Nitric oxide is produced by reaction between excited atomic nitrogen and molecular oxygen
  - At low- and mid-latitudes, solar soft x-rays primarily provide the energy for producing excited atomic nitrogen
  - At high-latitudes, production is primarily due to precipitating energetic particles in the auroral regions
    - Ties nitric oxide production to space weather

Generation in the Polar Upper Atmosphere

$$N_2 + EPP \rightarrow N^* + N$$
$$N^* + O_2 \rightarrow NO + O$$

Loss Processes

$$NO + N(\,^4S) \rightarrow N_2 + O$$
$$NO + O_2^+ \rightarrow NO^+ + O_2$$
$$NO + h\nu \rightarrow N(\,^4S) + O$$

Catalytic Destruction of Ozone

$$NO + O_3 \rightarrow NO_2 + O_2$$
$$NO_2 + O \rightarrow NO + O_2$$

Downward Transport

The Stellar Occultation Technique

- Measurements of nitric oxide will be performed using the stellar occultation technique
  - Targeting an SNR of 1 on 2E15 cm^{-2} nitric oxide column density with 3 km altitude resolution
  - $\frac{I_{occ}}{I_{ref}} = \int_{bandpass} \exp(-\tau) d\lambda$
    - $\tau(\lambda, T) = \sigma(\lambda, T) N$
  - Requires very high precision measurements of star light over approximately 1 sec duration altitude bins

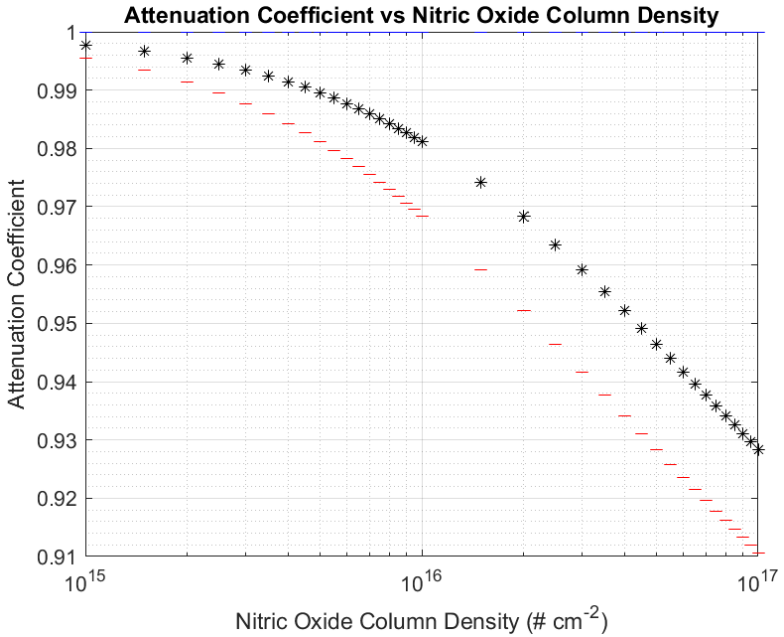

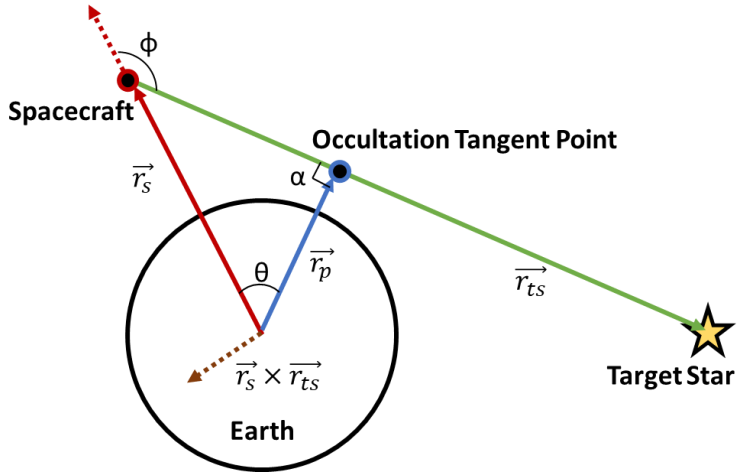

Instrument Overview

- To meet measurement sensitivity requirements in massively reduced SWaP budgets, must take advantage of several technology developments
  - Extremely narrow bandpass filter
    - FWHM between 1 and 2 nm, centered at 215 nm, in development with Materion
  - UV-specialized CubeSat compatible optics, provided by LLNL
    - 8.5 cm aperture, Cassegrain design
  - **Delta-doped EMCCD with UV-specialized AR coating**
    - Utilizing CCD201-20 from Teledyne e2v
    - Camera electronics and delta-doping process from NASA JPL
    - **Enables the use of photon counting operation to virtually eliminate read noise from the measurement**

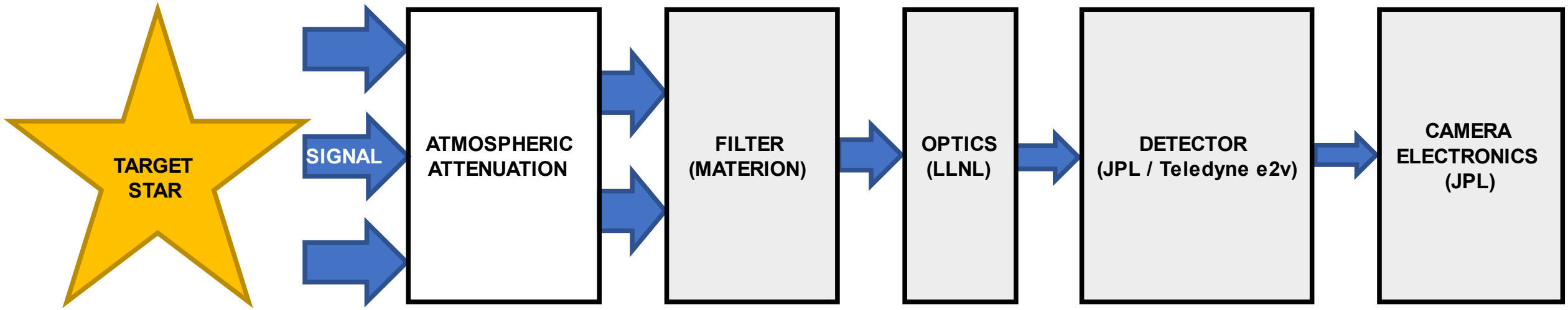

The EMCCD

- EMCCD => Electron Multiplying Charge Couple Device
  - Sometimes called a Low Light Level (L3) CCD
- An extension of standard CCD technology that includes a multiplication register for applying high gain to the signal before readout
- Composed of a large array of individual pixel elements
- Charge is generated by incoming photons through the photoelectric effect
  - The **interacting Quantum Efficiency (iQE)** characterizes the percentage of photons that successfully produce a charge within a pixel
  - **Quantum Yield (QY)** characterizes the number of electrons produced per interacting photon
    - Silicon energy band gap of 1.14 eV limits interactions to wavelengths ~< 1100 nm

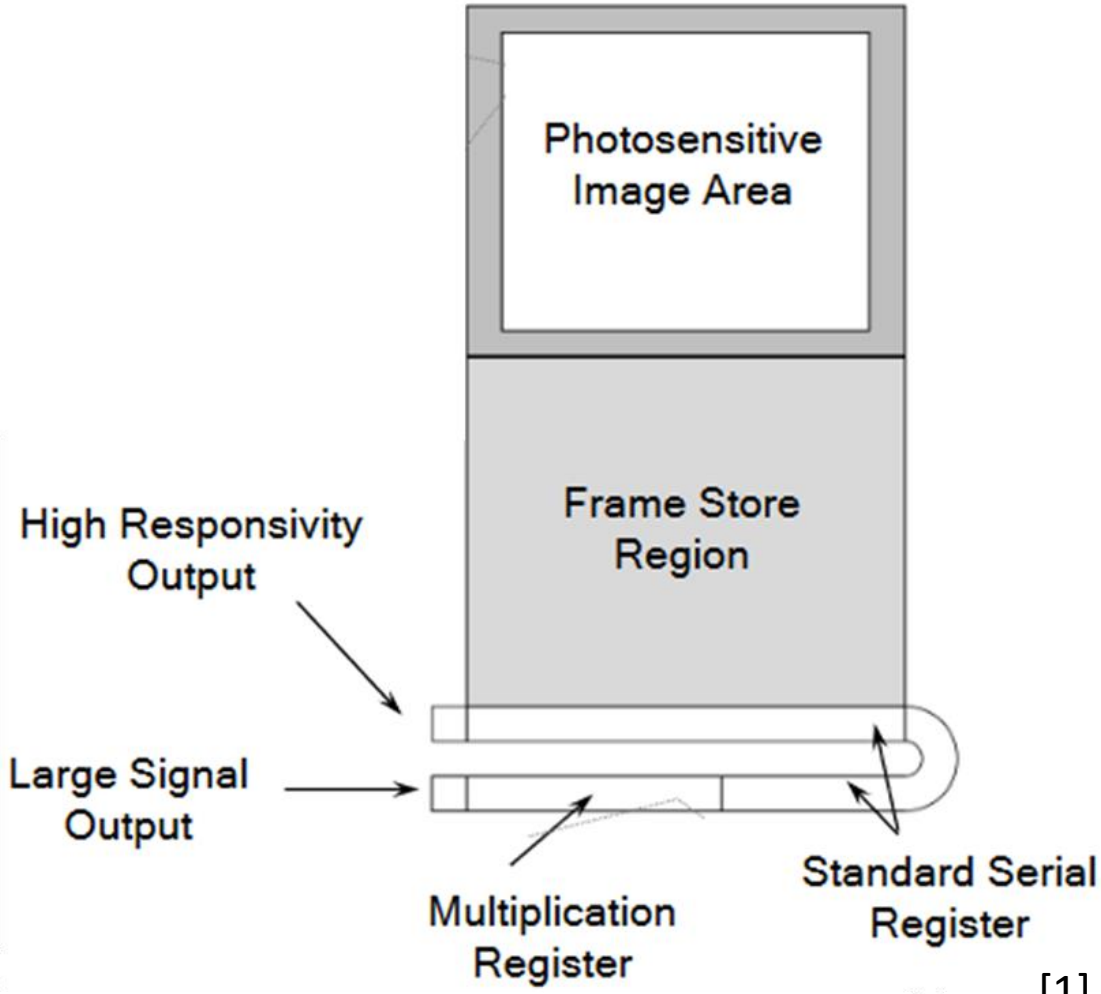

[1]

Charge Transfer

- The generated charge is collected into individual pixels on the array
- Charge is then marched out of the array through manipulating the potential within the pixels
- Efficiency of the charge transfer process is characterized by the **charge transfer efficiency (CTE)**
  - Poor CTE performance will “smear” the charge in the direction of transfer
- Charge is transferred out of the imaging section in parallel, but must be transferred in serial in the readout register
- Charge measurement occurs at the output registers, where the number of electrons on the final pixel is sensed and taken through an output amplifier
  - Introduces read noise to the measurement
  - The **camera gain constant** provides the conversion between the number of electrons and the recorded digital number (DN)

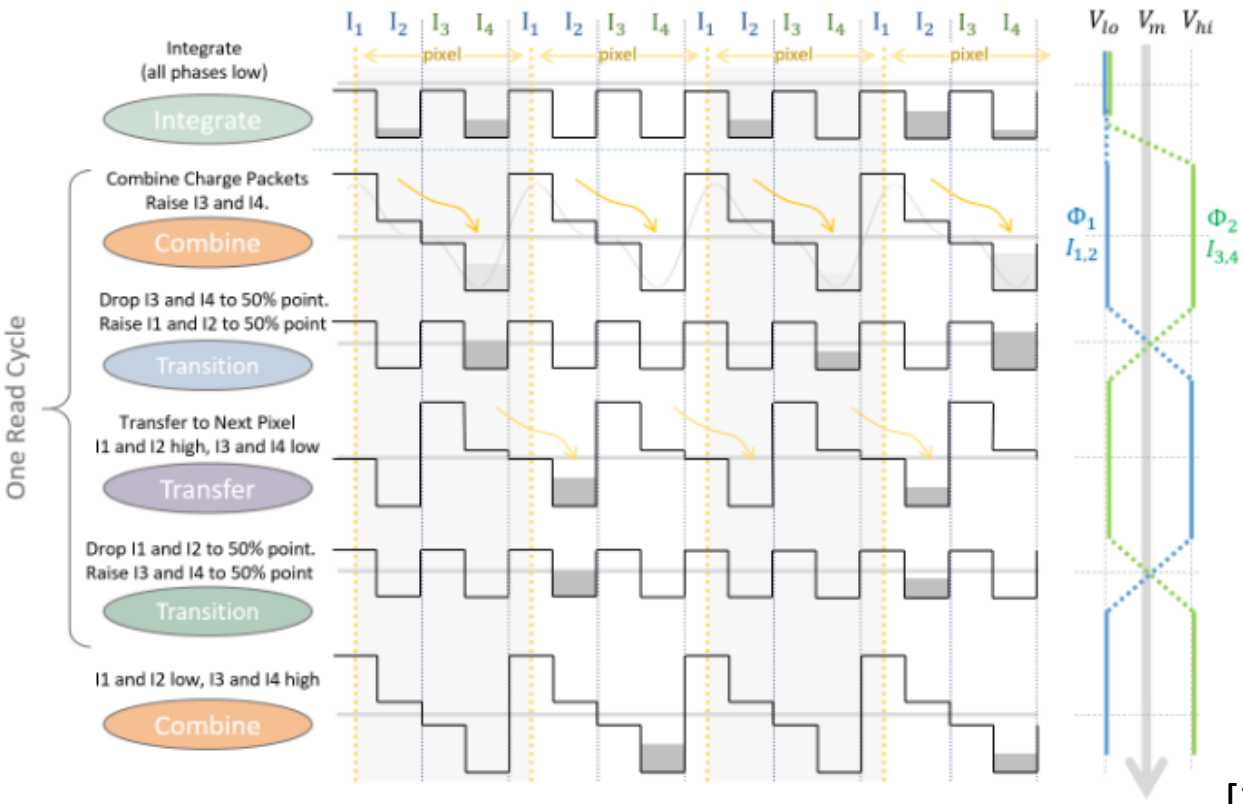

[2]

Electron Multiplication

- The EMCCD expands on the standard CCD architecture by including an additional output register with multiplication elements
- Transfer through the multiplication elements occurs as before, but introduces a very high voltage (~40 V) under the Rϕ2HV stage
  - Accelerates the electrons within the charge cloud to cause impact ionization to occur
- Each stage (of a total n) has a probability for multiplying the signal, p, providing a mean gain, G
  - $G = (1 + p)^n$
  - $P(x) = \frac{x^{n-1}\exp(-\frac{x}{G})}{G^n(n-1)!}$

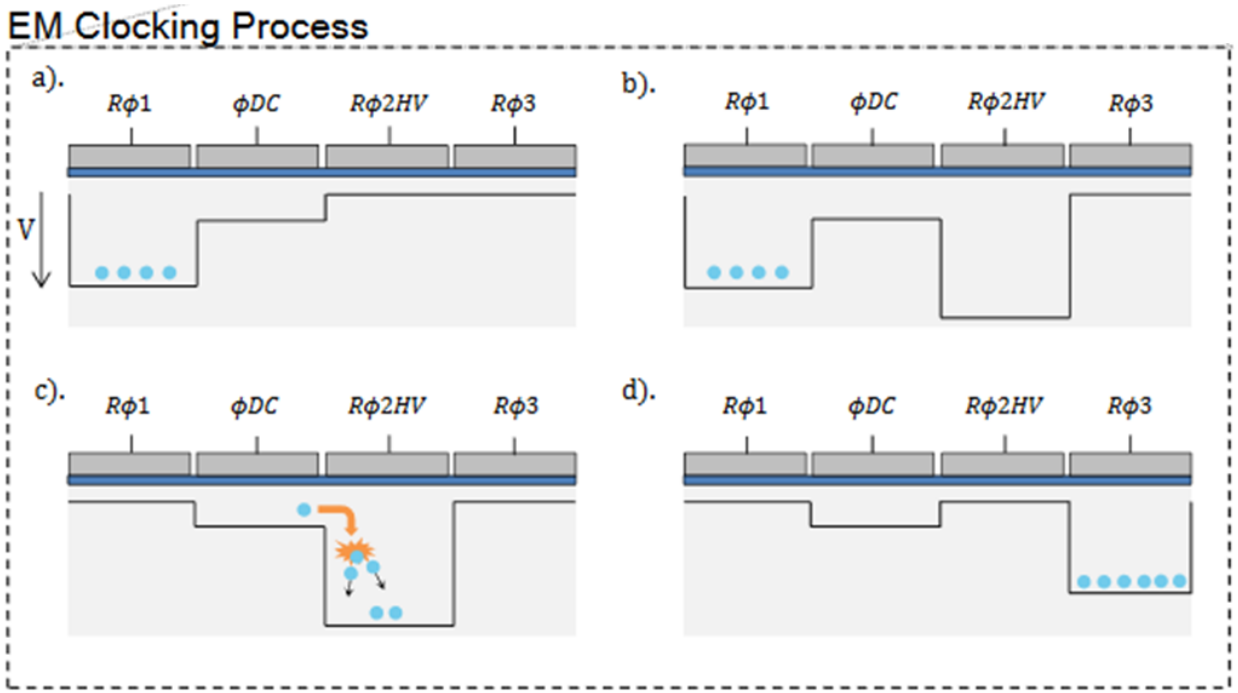

[1]

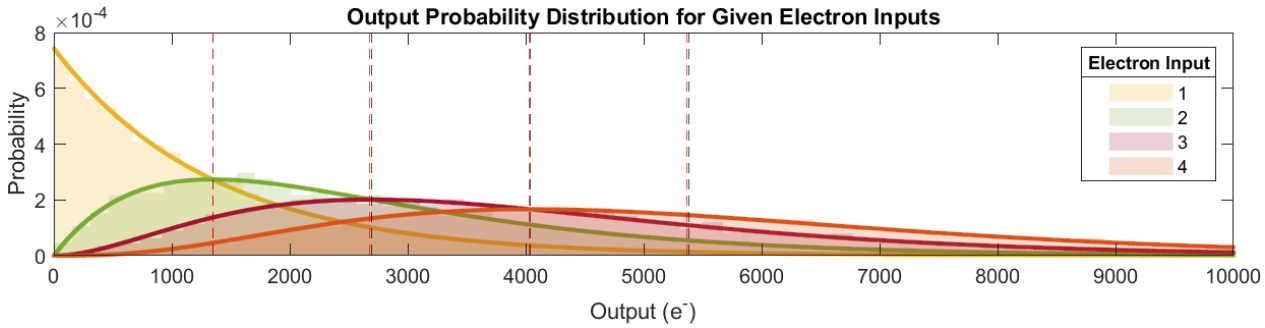

Important Noise Sources

- **Shot noise**
  - Due to the inherent statistical uncertainty in the arrival of photons incident on the detector
- **Dark current**
  - Thermal energy of electrons within the CCD bulk material is sometimes high enough to cross the band gap, adding them to the charge cloud
  - Mitigated by cooling the detector
- **Read noise**
  - Applied during the read-out process
- **Clock – Induced – Charge (CIC)**
  - During the pixel clock-out process, holes within the CCD material are also accelerated and can create charge through impact ionization
- **Fano Noise**
  - Noise due to variation in the number of electrons produced by a photon of a given energy

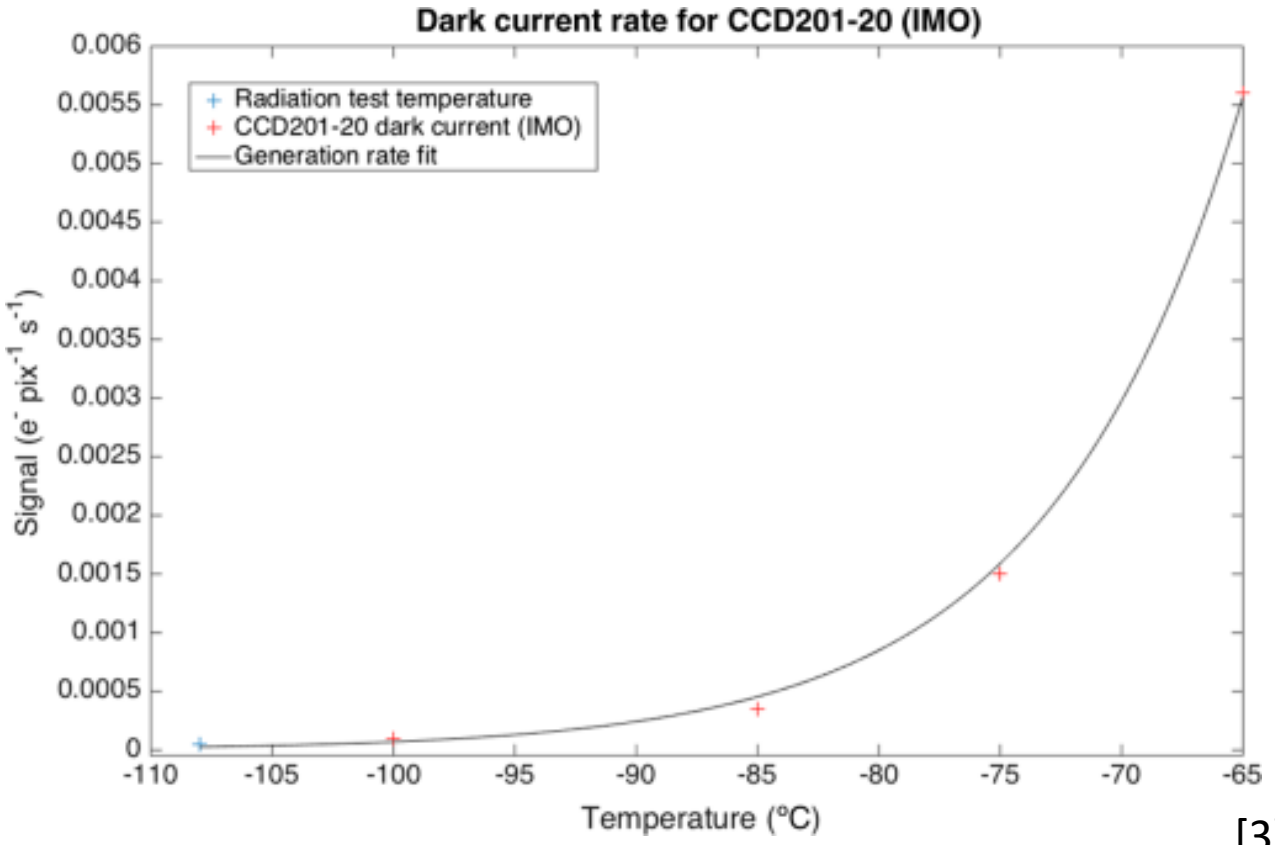

[3]

Photon Counting

- Take advantage of electron multiplication to effectively remove the instrument read noise from the measurement via thresholding
  - Application of the threshold results in undercounting due to some real signal falling within the read noise
  - To avoid coincidence losses, must limit the signal level to less than 0.2 photons per pixel per readout

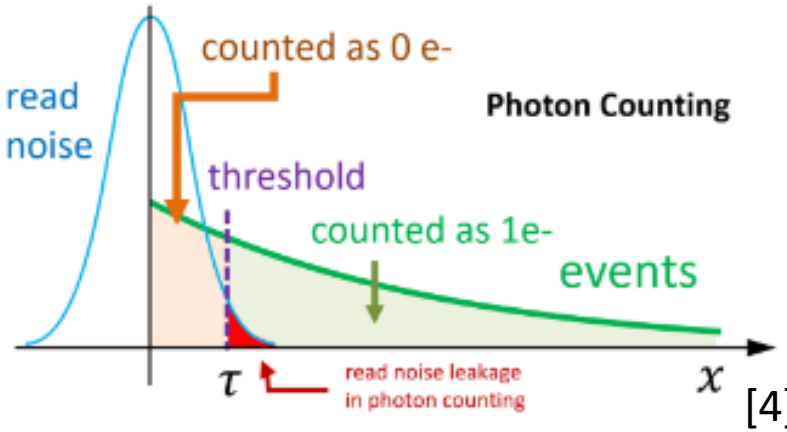

[4]

Photon Counting

$$SNR = \frac{D_{prob}\, S}{\sqrt{D_{prob}(S + T + N_f C)}}$$

Analogue Mode with EM Gain

$$SNR = \frac{S}{\sqrt{ENF^2(S + T + C) + N_p(\frac{\sigma_r}{G})^2}}$$

Standard Readout

$$SNR = \frac{S}{\sqrt{S + T + C + N_p\sigma_r^2}}$$

Star	Photon Counting	Analogue	Standard
a CMa	248.30	191.09	6.86
a Leo	74.75	72.44	1.04
a Vir	249.52	191.93	6.92
b CMa	149.19	123.11	2.89
d Sco	84.03	78.86	1.22

Operation in the Space Environment

- High energy particle environment presents a challenge for EMCCD operation
- High energy particles are able to generate a large number of electron – hole pairs as they travel through the detector
  - Enough to saturate the pixel and create long tails effecting entire columns in the imaging section (blooming)
  - Limits total integration time in the space environment
- Can also permanently damage the device
  - Degradation if CTE, increase in dark current and CIC rates, creation of trap sites
  - Trap sites introduce additional energy levels within the bandgap that can trap photoelectrons

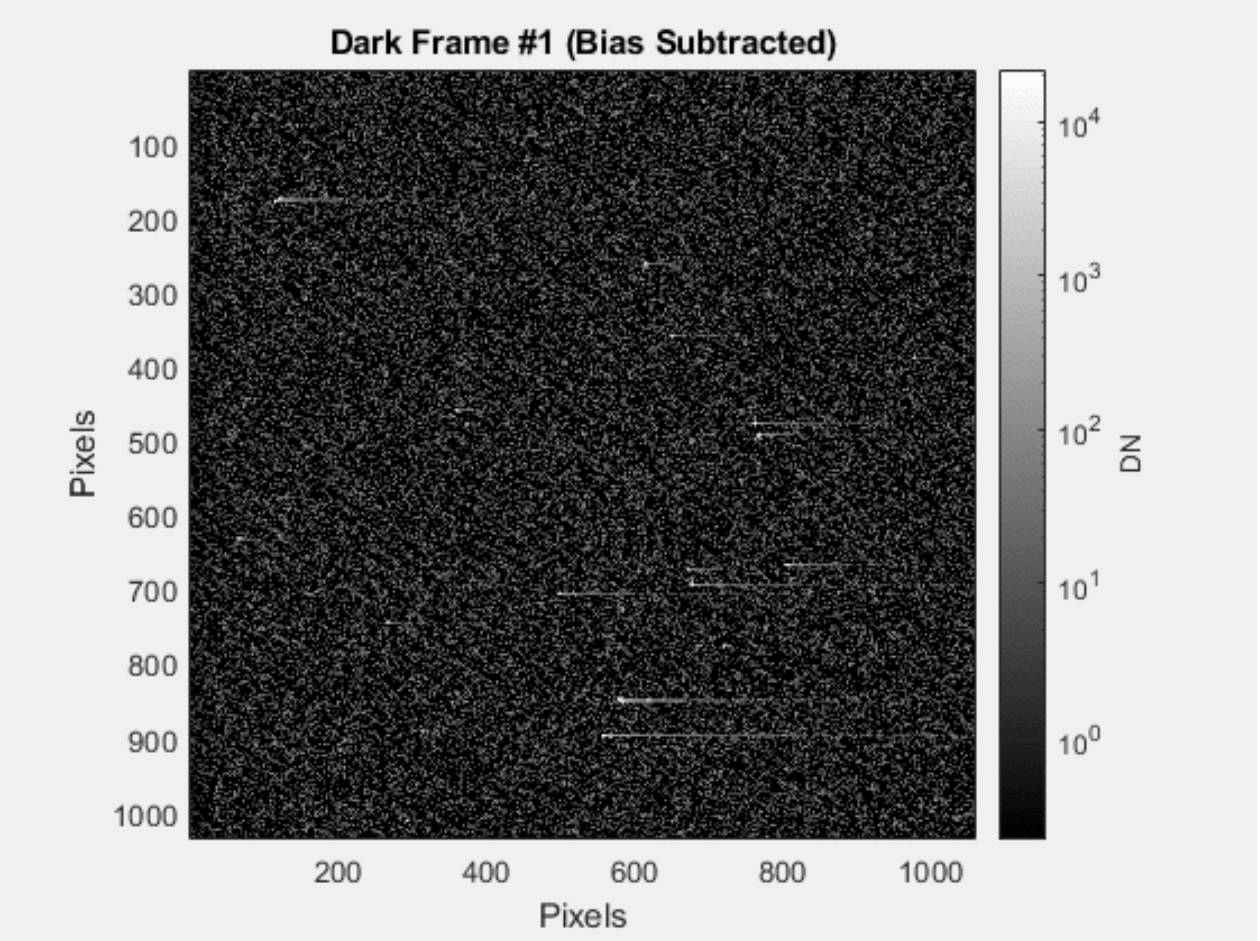

Model Overview

- (EM)CCD model has been implemented in MATLAB to simulate detector operations at high fidelity
  - Charge Generation
  - Charge Collection
  - Charge Transfer
  - Charge Measurement
  - Noise Processes
- The detector is modelled at the individual pixel level
  - Modelling of pixel level defects
  - Explicit definition and execution of read-out sequences
- Model is “physics informed”

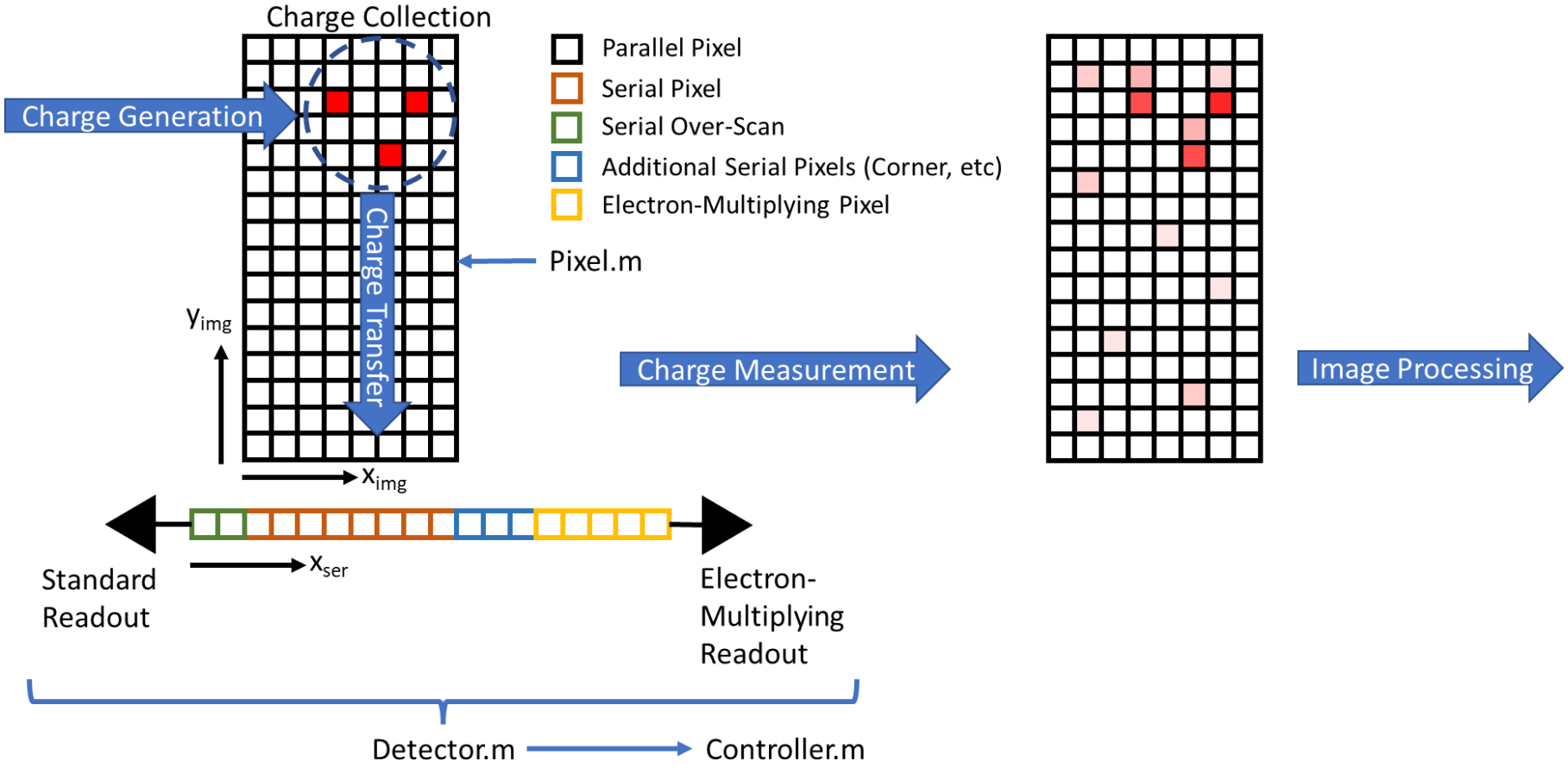

Pixel

- Lowest level representation is the Pixel class
- Used to store information regarding pixel state and properties
- By setting different properties, different pixel functions can be modelled (image section, transfer section, serial pixel, etc)
- Amount of charge is stored in the charge cloud for each pixel
- iQE and QY are stored as wavelength dependent values

Property	Description
Interacting Quantum Efficiency	Determines the number of incident photons that generate an e-h pair (0 – 1)
Quantum Yield	Determines the probability of an interacting photon producing a second e-h pair (≥ 1)
Full Well Capacity	Sets the capacity of each pixel (e^-)
Charge Transfer Efficiency	Determines the amount of charge transferred (0 – 1)
Dark Current Rate	Dark current generation rate ($e^- s^{-1}$)
Clock – Induced – Charge Rate	Mean CIC rate, **defined per transfer** (e^- $transfer^{-1}$)
Multiplication Probability	Probability of electron multiplication per electron within the pixel (0 - 1)

Constant	Value
Average e-h pair production energy	3.65 eV
Fano Factor for Silicon	0.1

Detector

- Contains Pixel object arrays representing the parallel and serial sections
- Coordinates transfer of charge between pixels
- Allows for setting pixel level properties within the array to simulate non-uniformities and defects
  - Properties can be set independently between the parallel and serial sections
- Both standard and EM outputs are modeled

Property	Description
Parallel Section Length / Width	Size of the parallel section (Pixels)
Serial Register Overscan	Number of overscan elements in the serial section before the standard readout (Pixels)
Serial Additional Elements	Number of elements in the serial register between the image section and EM elements (corner, etc.) (Pixels)
Serial Multiplying Elements	Number of electron – multiplying elements in the serial register (Pixels)
EM / STD Read Noise	RMS read-out noise for the read-out amplifier (e^-)
EM / STD Read Bias	Bias applied to the read-out (e^-)
Mean Gain	Sets the mean gain for the detector. Along with the number of multiplying elements, calculates the correct multiplication probability for individual pixels.

Controller

- Contains and coordinates access to a Detector object
- **Coordinates the readout sequence of the detector**
- Used to control horizontal and vertical frequencies, application of the camera gain constant, and digitization of the read-out
- Supports modification of properties at the pixel level for degrading dark current generation and CTE performance in the parallel and serial sections

Property	Description
Camera Gain Constant	Controls conversion between e^- to DN at the detector read-out ($e^- DN^{-1}$)
ADC Resolution	Sets the number of bits used by the ADC (# bits)
ADC Offset	Sets any offset in the ADC corresponding to the 0 level of the readout (DN)
Vertical Frequency	Sets the frequency for vertical transfers (Hz)
Horizontal Frequency	Sets the frequency for horizontal transfers (Hz)

Code Overview

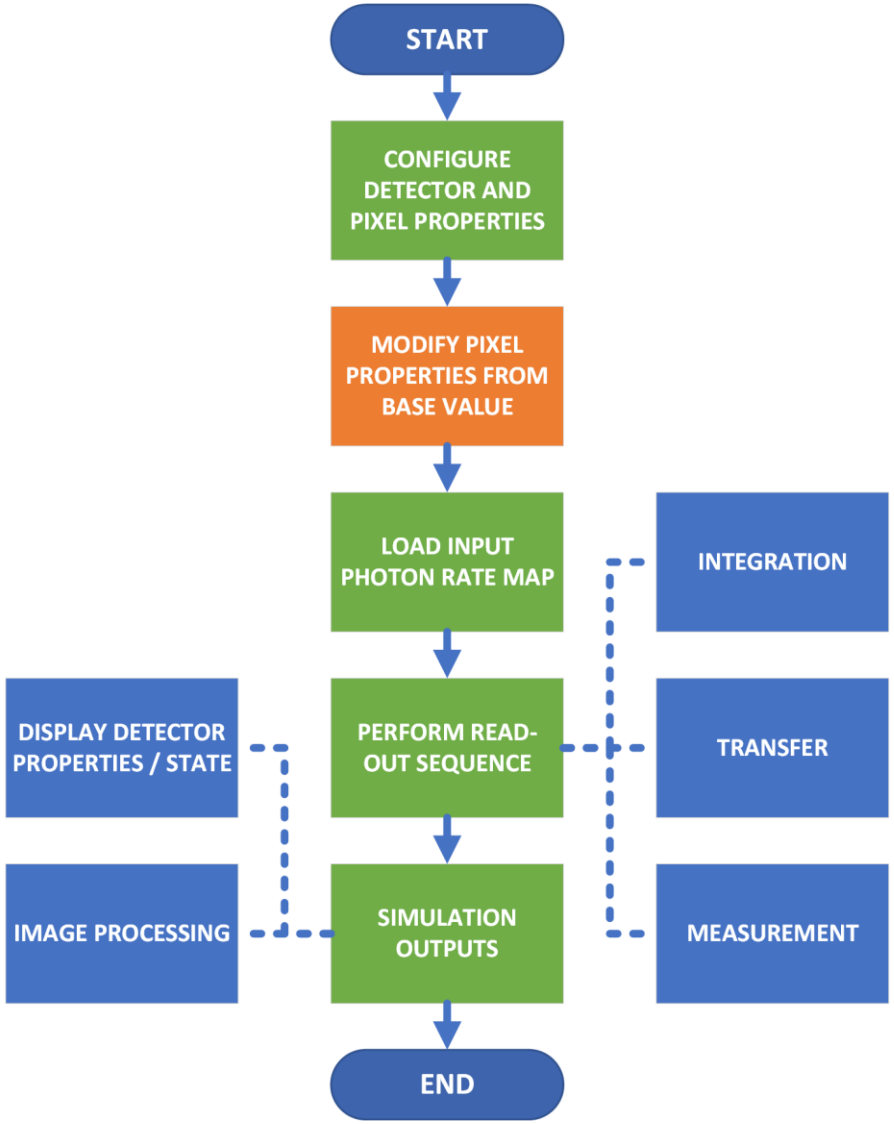

Process	Model	Notes	Reference
Incoming Photons	Poisson Distribution	Shot Noise	
Photon Interaction	Binomial Distribution	Interacting Quantum Efficiency	
Quantum Yield	Binomial / Normal Distribution	Fano Noise	[5, 6, 7, 8]
Dark Current	Poisson Distribution		
CIC	Poisson Distribution		
Charge Transfer Efficiency	Binomial Distribution		
Electron Multiplication	Binomial Distribution	Captures ENF	[9]
Read Noise	Normal Distribution		

Charge Generation

- **Incoming Photons**
  - Specified for a specific wavelength
    - Multiple wavelengths of light can be incident on a detector simultaneously
  - Implemented as **map of incoming mean photon incidence rate** over the parallel section of the array
    - Specified in mean photons per seconds
  - Charge is generated for all steps of the process for which a finite time interval is defined
    - Includes integration times and during vertical and parallel transfers
  - The number of photons incident on a pixel over a time interval is determined by multiplying the mean photon incidence rate by the time interval, then using this mean number of incident photons to feed a Poisson random number generator to simulate **shot noise**
  - The number of interacting photons is then determined by the **interacting quantum efficiency**
    - A binomial distribution is used, where each interacting photon is a “trial”, and the probability of successfully interacting with the pixel is set by the interacting quantum efficiency.
    - Interacting quantum efficiency is input as a wavelength-dependent vector
      - Interpolation can be done using a ‘linear’ or ‘nearest’ method

Charge Generation

- **Fano noise** is incorporated by allowing the interacting photons to generate multiple electron-hole pairs within the pixel through simulation of the **quantum yield**
  - For λ > 350 nm
    - Quantum Yield is set to 1
  - For 123.9 nm < λ ≤ 350 nm
    - Use data from [2] to determine the quantum yield through linear interpolation
    - Implement model in [4] to allow the photon to generate up to 2 additional electrons.
    - $QY = 1 + P_m + P_m^2$
      - P_m is the probability of generating an e-h pair
    - Modelled as a Bernoulli process where the number of additional e-h pairs generated is determined by a binomial distribution
  - For λ ≤ 123.9 nm
    - Use equations from [1, 3] to calculate mean quantum yield and FWHM for photons with energy > 10 eV
    - $\eta_i = \frac{E(eV)}{E_{e-h}}, \delta E = 2.355\left(\frac{F\,E(eV)}{E_{e-h}}\right)^{\frac{1}{2}}$
      - *F* - Fano Factor
      - *E(eV)* – Incoming photon energy
      - $E_{e\text{-}h}$ – 3.65 eV per e^-
    - Calculated FWHM and mean of quantum yield is used to inform a gaussian random number generator

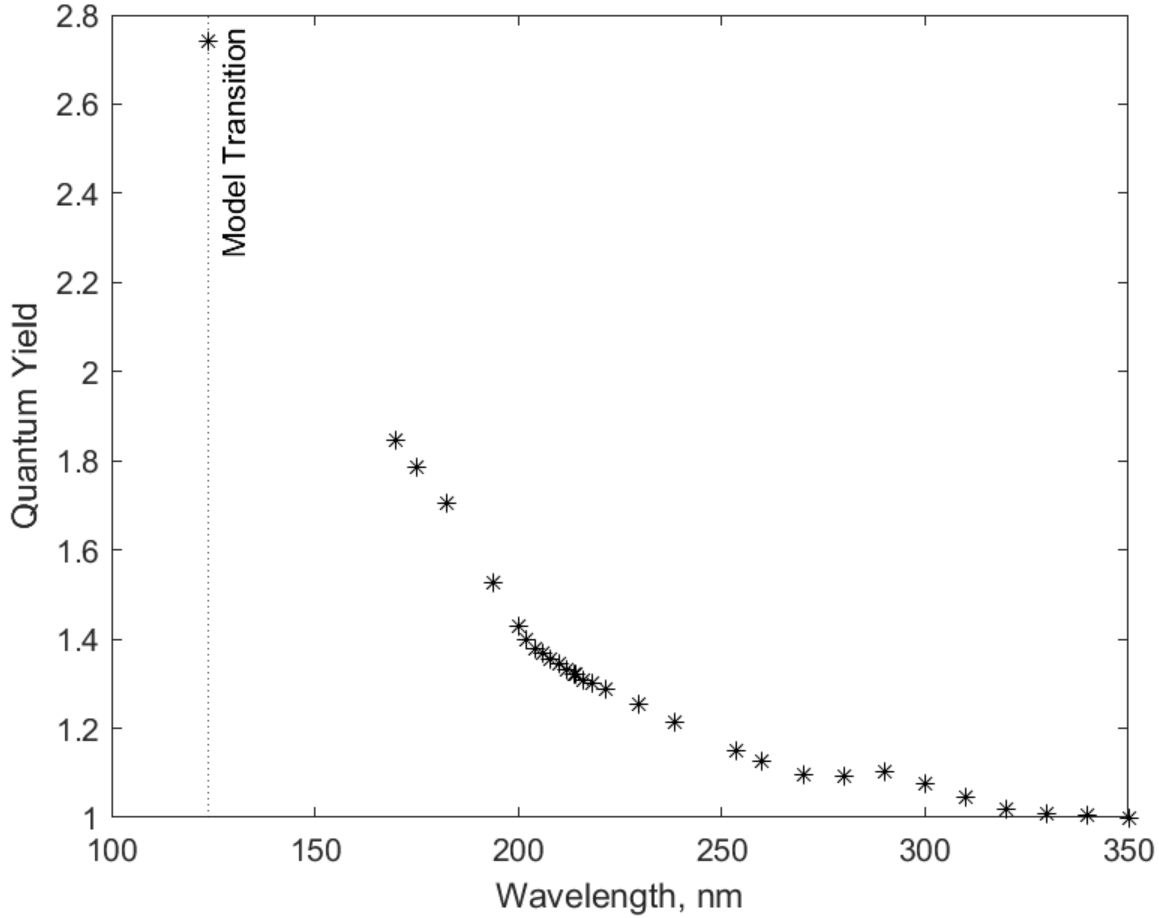

Charge Generation

- **Dark Current**
  - The mean dark current generation rate, along with the time interval, are used to inform a Poisson distribution to generate dark current over each interval

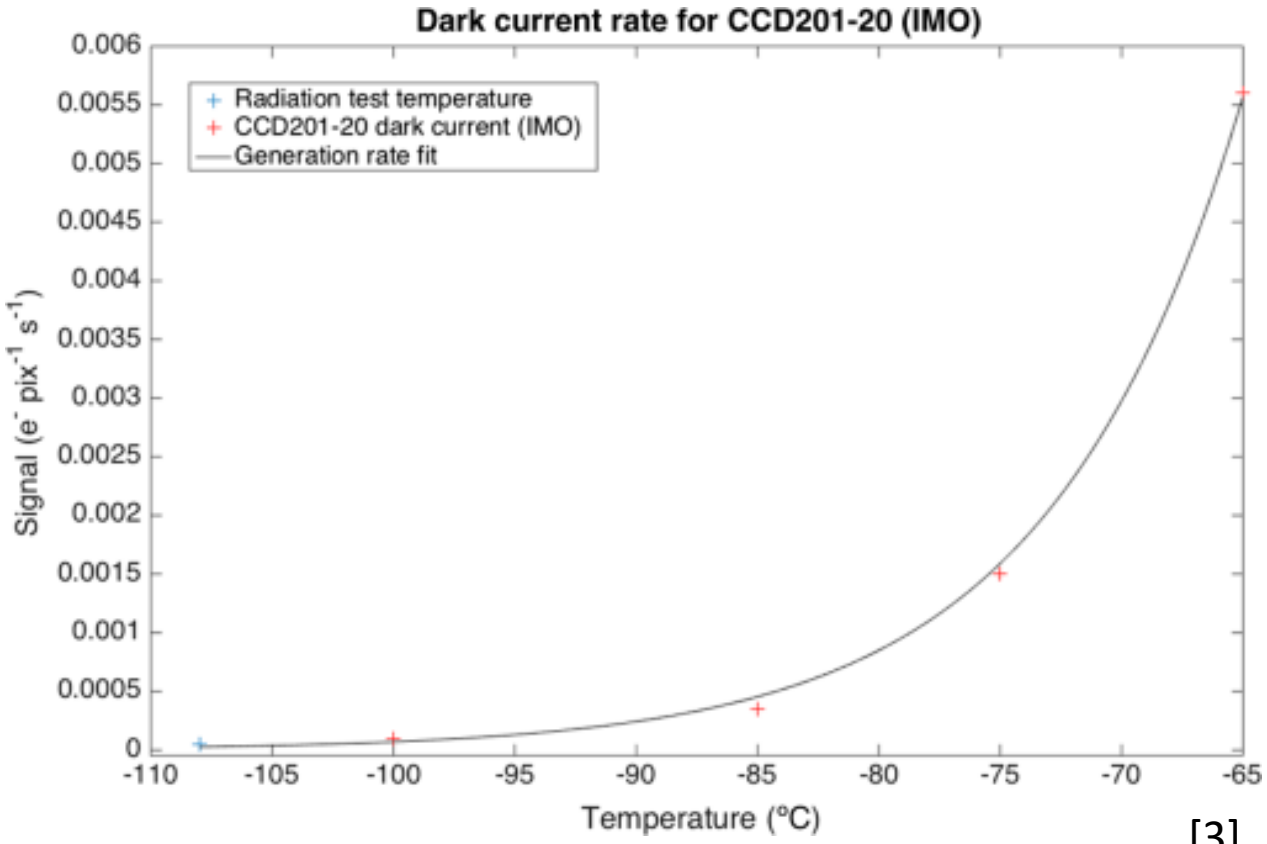

[3]

Charge Transfer

- Coordinated by the Detector class
- Charge can be transferred in the forward and reverse directions in the parallel and serial sections
- Before each transfer, charge is generated in the parallel and serial section to best reflect the total signal levels
  - Based on timing given by vertical and horizontal frequencies
- Amount of charge transferred is based on the 'from' pixel **CTE**.
  - Modelled using a binomial distribution, where each electron is a "trial," and the probability of being successfully transferred is given by the CTE
  - **CIC** is added to the out-going charge cloud during each transfer
- Charge multiplication (for those pixels with multiplication set to a non-zero value) is applied upon transferring that charge into the pixel

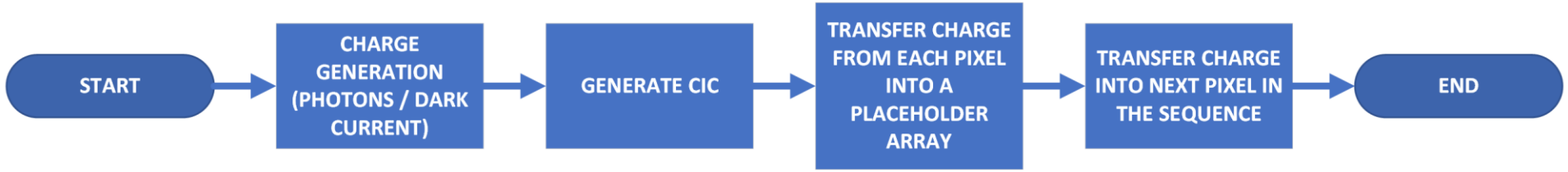

Charge Multiplication

- Based on description of **electron multiplication** process and statistics in Basden et al., 2003 [2].
- When transferring charge into a pixel with a multiplication probability greater than 0, a binomial distribution is used to determine which electrons are multiplied using the multiplication probability as the probability of success
  - The multiplied electrons are then added to the charge cloud
  - Variability of multiplication captures the **Excess Noise Factor** (ENF)
- Plot below shows simulation of electrons multiplied through multiplication elements
  - Shaded histograms represent simulation output
  - Solid line plots shows analytical expression provided for output probability in [9]
  - Red dashed lines show the simulation mean output
  - Black dashed lines show the calculated mean output

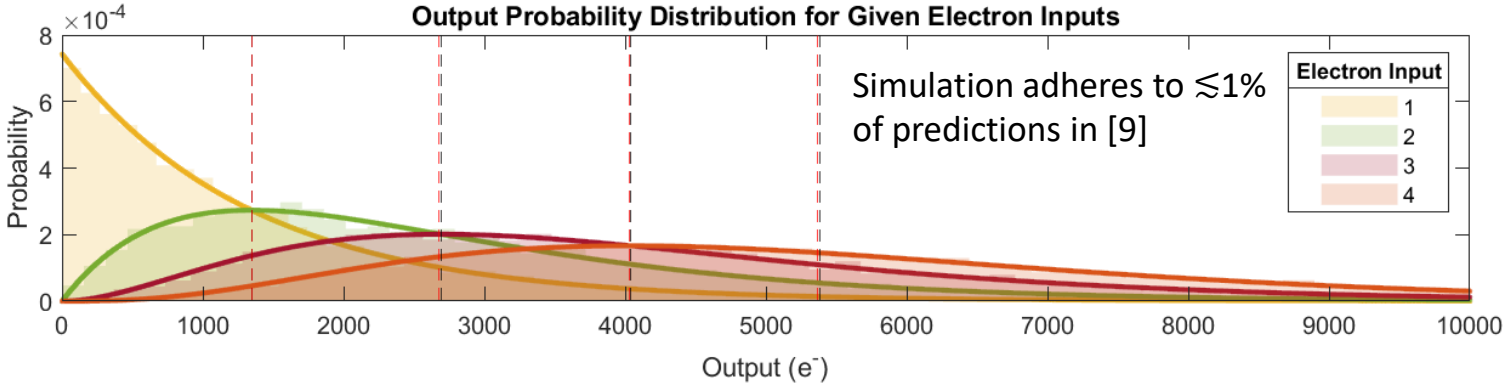

Property	Value
Multiplication Probability	0.012
Number of Multiplication Elements	604
Calculated Mean Gain	1345.95
Number of Trials per Input	10000

Charge Measurement

- Charge measurement is accomplished at the EM or standard readout register, whichever is being used
- **Read noise** is applied using a normal distribution (variance as specified in the detector configuration)
- A **bias level** can also be applied to the read-out
- Measurement is completed as part of a serial transfer where charge is moved out of the final pixel
- The **camera gain constant** and **digitization** is applied by the Controller object

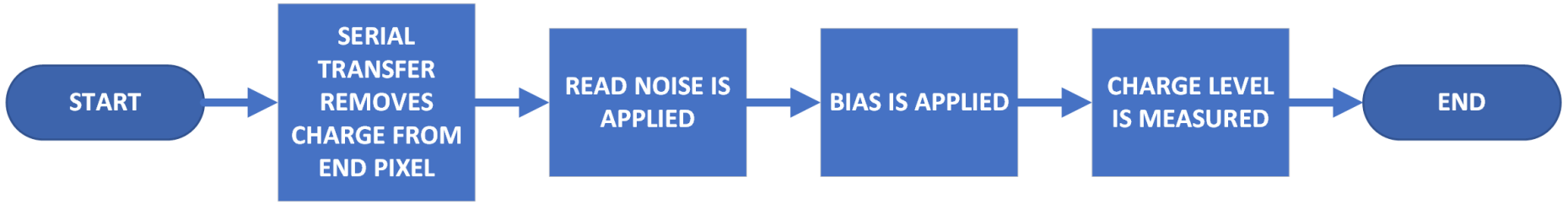

Assumptions & Limitations

- CCD response is linear across pixel charge level
  - Pixel properties are not dependent on charge level, non-linearity is not modelled
- Charge collection is assumed perfect
- Charge diffusion is not modelled
- Pixel size does not impact pixel properties
  - Pixel properties (such as dark current, charge diffusion, light gathering area, etc) are not explicitly tied to the provided size of the pixel

Model Operation

- Model is operated through a driver function that specifies the set-up parameters for the pixels, detector, and controller

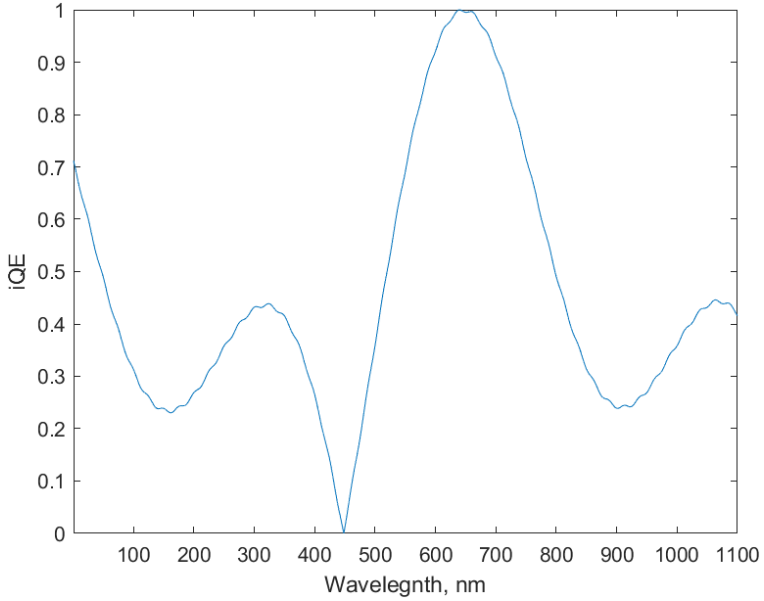

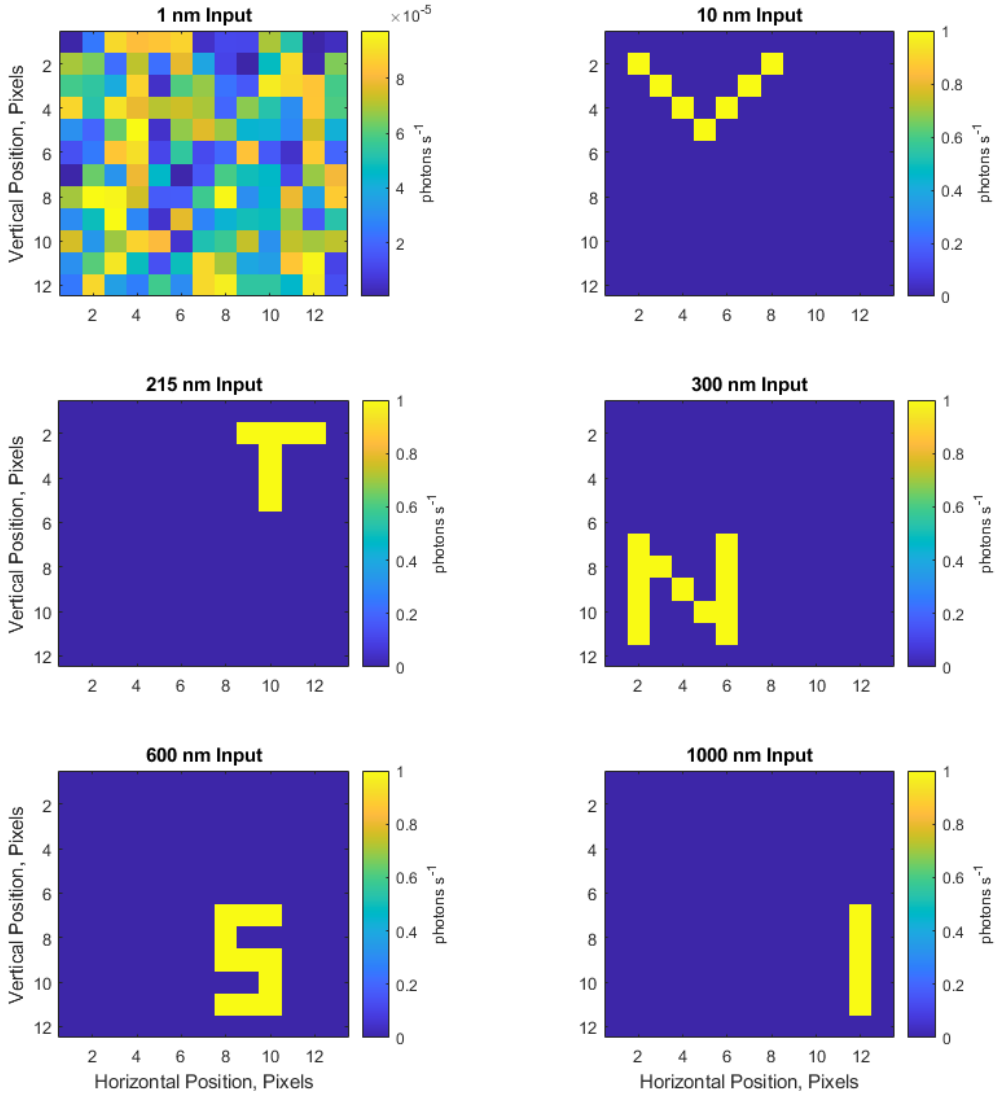

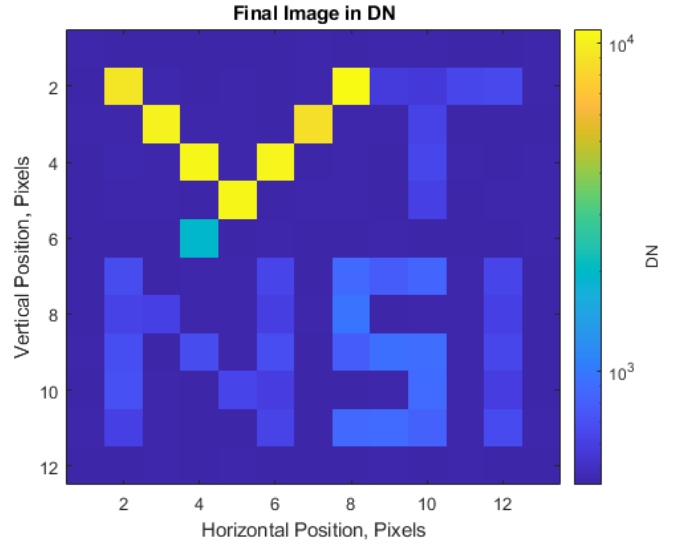

Model Operation

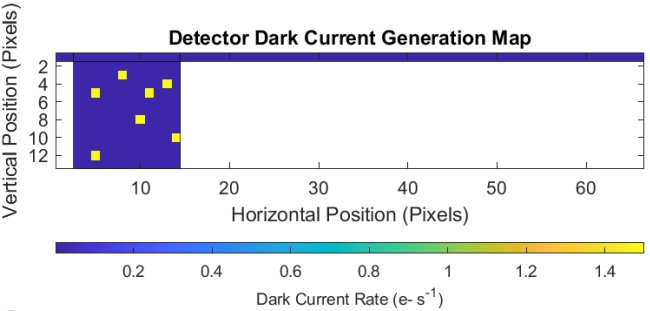

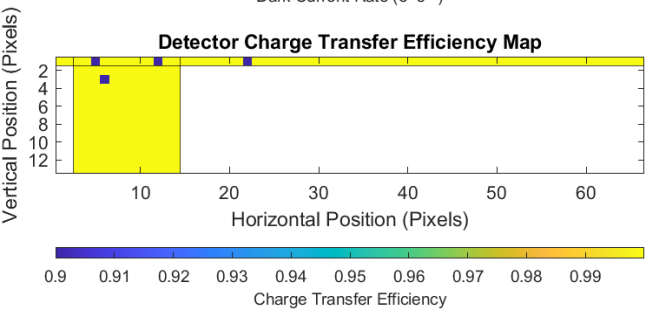

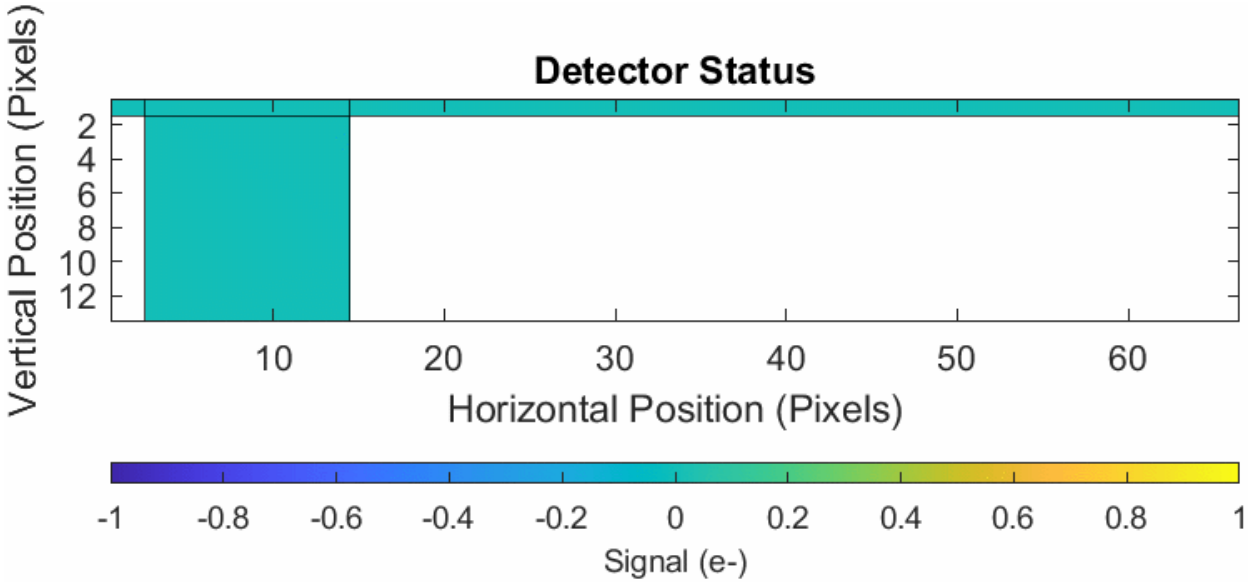

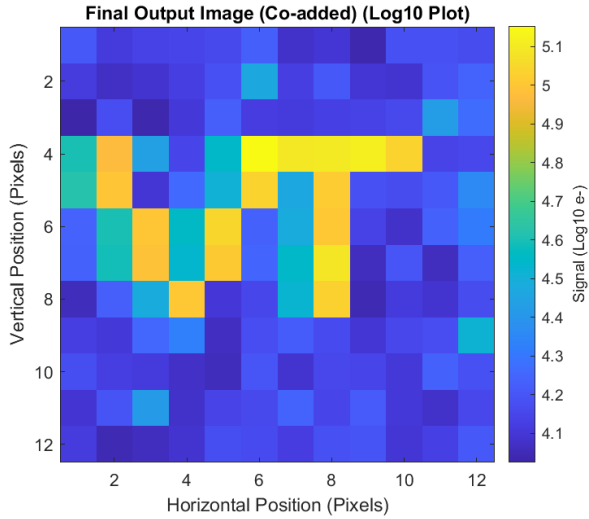

Model Validation – Camera Characterization

- A Nuvu EM N2 camera equipped with a Teledyne e2v CCD201-20 was characterized to provide validation data for simulated characterization of the EMCCD model
  - Camera cooled to -85 °C using LN2
- Collected data for:
  - Bias
  - Photon Transfer Curve
  - CIC
  - Dark Current
- Camera was operated at 10 MHz horizontal frequency, 1 MHz vertical frequency using the EM output register
  - Corresponds to the default profile 1 in the CCCP software suite

Bias Data

- Collected 144 full frames using a set integration time of 0 s
  - Effective readout time of ~120 ms
  - Gain set to 1
  - Data collected with cap on and shutter closed
- Note the use of the median bias frame to guard against impact of transient events
  - Adopted throughout characterization effort

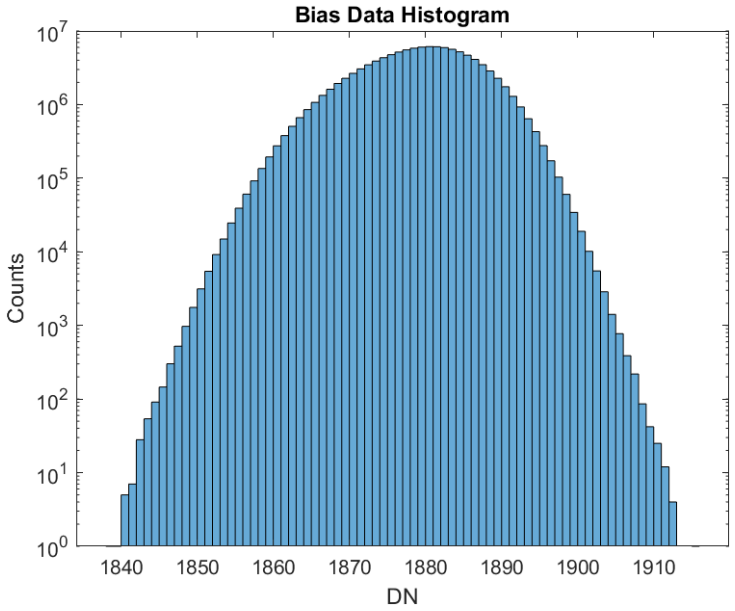

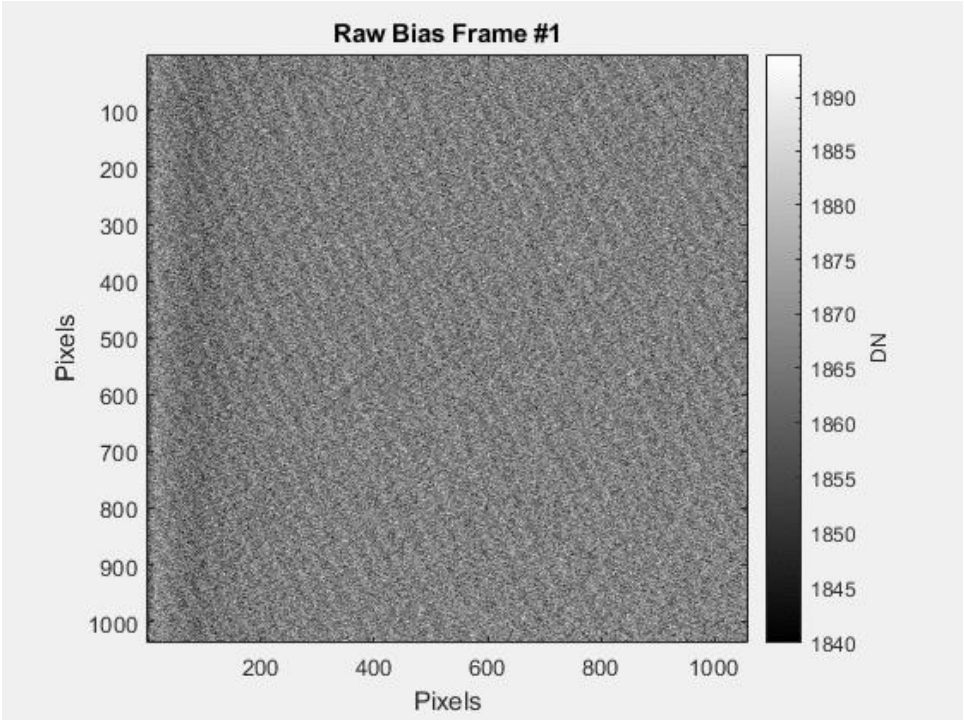

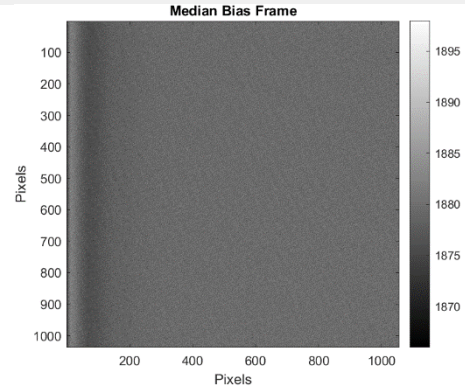

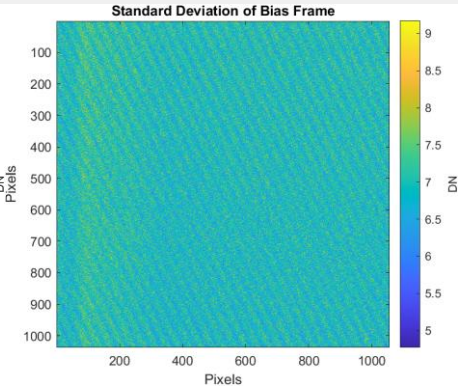

Photon Transfer Curve

- Collected full frames using variable background light and integration times to populate the signal vs noise curve
  - Gain set to 1
  - Data collected with cap off and shutter open
- Utilized Equation 2.8 in Janesick, 2001 to estimate the camera gain constant, *K*, from the linear portion of the log-log plot
  - $K = \frac{S(DN)}{\sigma_S^2(DN) - \sigma_R^2(DN)}$
  - Where S is the mean signal level of the frame, σ_S is the noise of the frame and σ_R is the read noise
  - The signal level was determined by removing the bias from the frame and taking the mean pixel signal level over the frame
  - Noise on each frame was determined by finding the standard deviation of all pixel signal levels over a difference frame

Parameter	Estimation
Read Noise (RMS)	5.2210 DN (92.798 e^-)
Camera Gain Constant	17.7740 e^- DN^{-1}

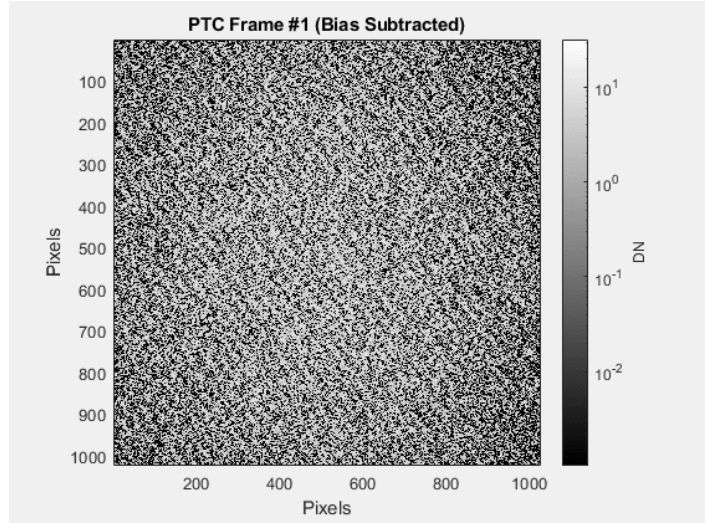

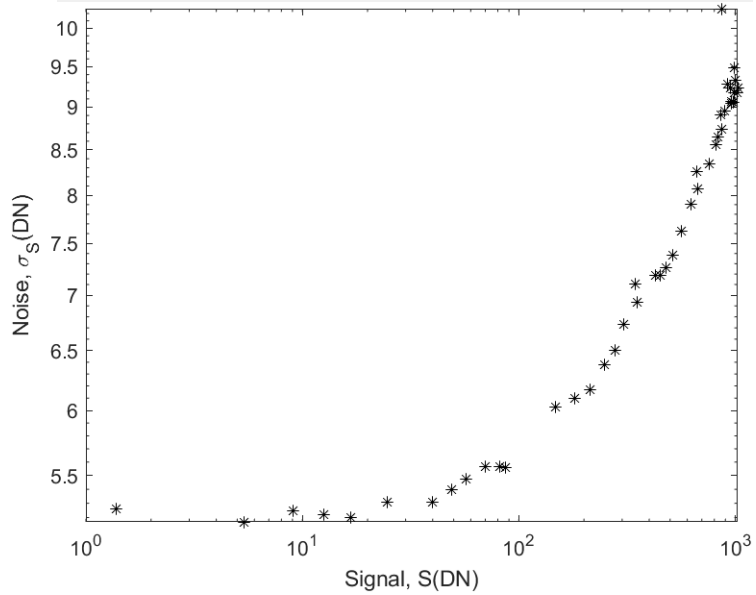

CIC Data

- Collected 1000 full frames using a set integration time of 0 s and gain of 1000
  - Effective time of ~120 ms
  - Low integration time makes dark current contribution negligible
- The bias frame subtracted from the CIC data was determined by taking the median pixel value over all 999 frames considered in the analysis
  - Bias level for the CIC data was significantly different than Bias data collected when gain was set to 0.
  - Median value was used over the mean to limit the impact of high signal events (muon strikes, amplified CIC electrons)
- Data collected with cap on and shutter closed

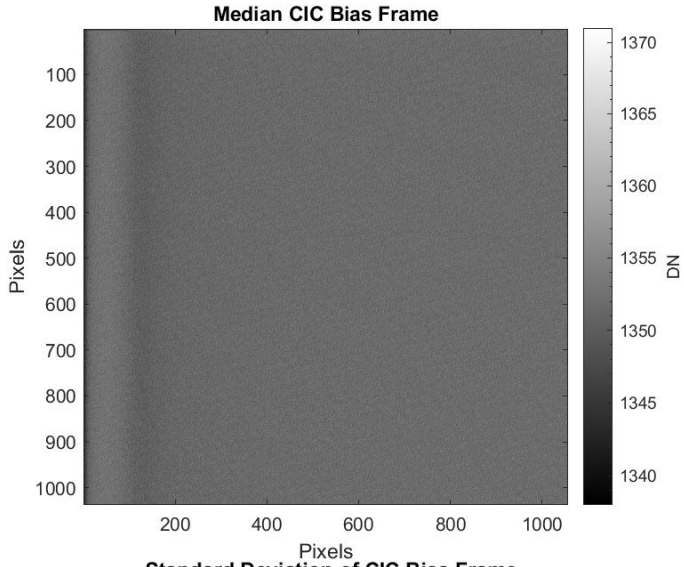

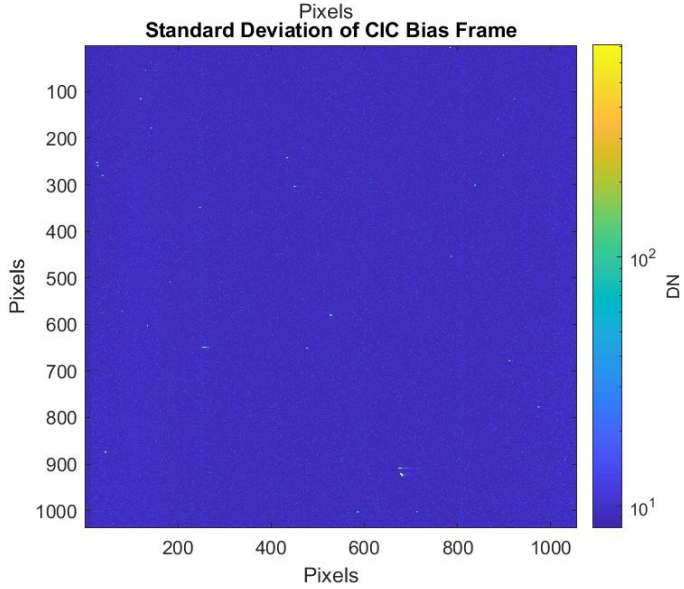

CIC Data

- The CIC rate is found using the technique described in "Extreme Faint Flux Imaging with an EMCCD" by Daigle et al., 2009
  - Output of the gain register is described by a PDF
  - $P(x,n,G) = \frac{x^{n-1}\exp\left(-\frac{x}{G}\right)}{G^n(n-1)!}$
    - x: Output of the gain register
    - n: Input to the gain register
    - G: Mean gain
    - When n = 1, this simplifies to the exponential distribution function
  - Use the data between 6 and 20 times the read noise to fit the data to exponential distribution function
    - Avoid impact of read noise
    - Also allows the gain to be determined
  - Can determine the CIC rate through:
    - $CIC_{rate} = \frac{N_{6\sigma\rightarrow 20\sigma}}{N_{frames}\int_{6\sigma}^{20\sigma} p(x,n,G)dx}$
    - $N_{6\sigma\rightarrow 20\sigma}$ is the count between 6 and 20 times the read noise RMS value
    - N_{frames} is the number of frames within the data set
    - $\int_{6\sigma}^{20\sigma} p(x,n,G)dx$ is the portion of the CIC expected to be between 6 and 20 times the read noise. Note that for these integration limits, and assuming that n = 1, this simplifies to $\exp(-\frac{20\sigma}{G})(-1+\exp\left(\frac{14\sigma}{G}\right))$
    - CIC_{rate} is in DN pixel^{-1} fr^{-1}. Apply the camera gain constant to get into terms of e$^-$
- **Determined CIC rate of 0.0031 e$^-$ pix^{-1} fr^{-1}**
  - **Compare with 0.002 e$^-$ pixel^{-1} fr^{-1} given in the EM N2 datasheet for same temperature, gain, horizontal frequency parameters**
- **Gain estimate from model fitting: 995.382**

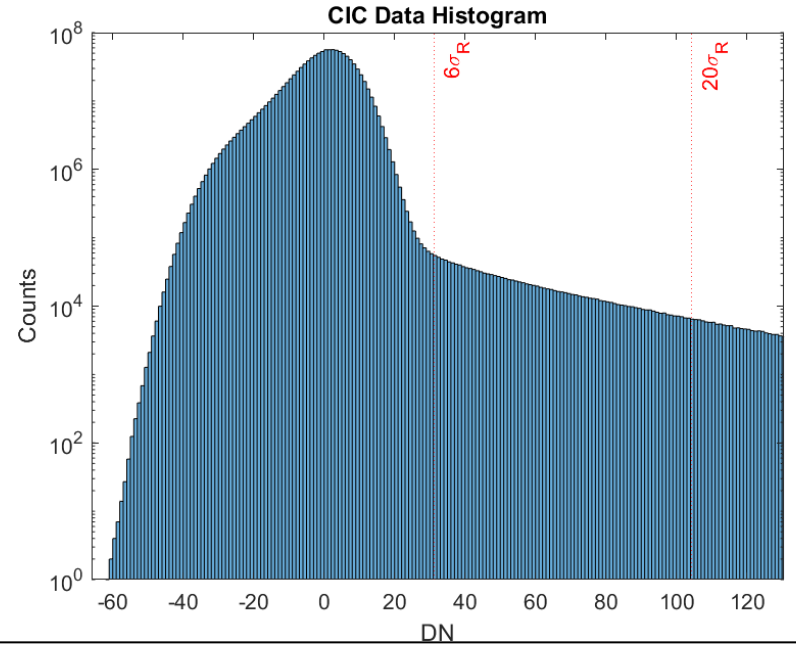

Note: The derived CIC rate is well below the 0.2 event pixel^{-1} fr^{-1} limit for minimizing coincidence losses in photon counting, so the assumption of n = 1 is appropriate.

Note: Simply applying photon counting will yield an undercount of the CIC (in this case, 0.0019 e$^-$ pixel^{-1} fr^{-1}), as a large portion of it is buried in the read noise.

Applying the detection probability of 61% for $\frac{G}{\sigma} = 10$, retrieves the correct estimate.

Dark Current Data

- Collected 144 full frames using a set integration time of 100 s and a gain of 1000
  - Data collected with cap on and shutter closed
- Same procedure used to find the CIC is used to determine the dark current rate
  - CIC rate is subtracted from the estimate to isolate the dark current component
  - To translate from per frame to per seconds, the value is divided by the integration time
- **Signal from muons striking the detector were not removed from the data**
- The bias frame subtracted from the dark data was determined by taking the median pixel value over all frames considered in the analysis
  - Bias level for the dark data was significantly different than Bias data collected when gain was set to 1.
  - Median value was used over the mean to limit the impact of high signal events (muon strikes, amplified dark electrons)

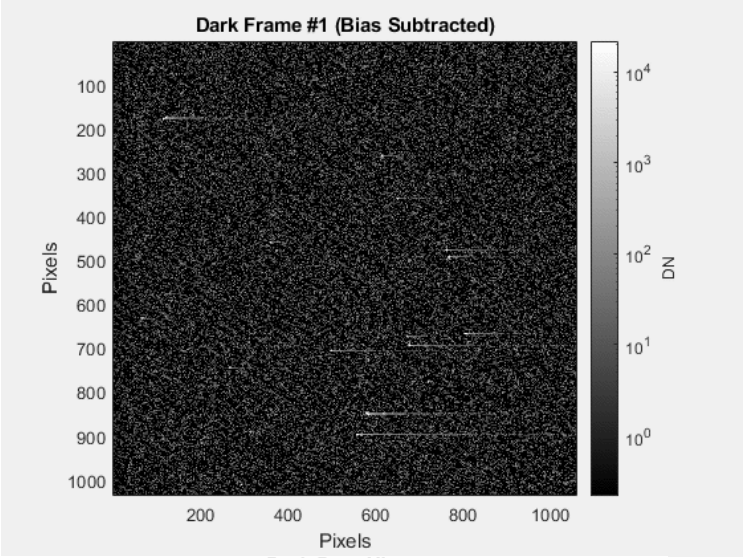

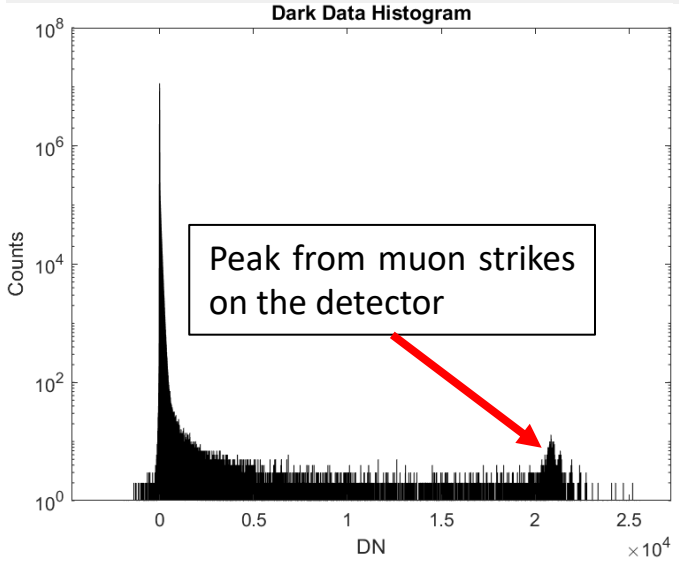

Dark Current Data

- Some “hot” pixels are observed on the detector
  - Row 198, Column 310
  - Line of hot pixels on Row 2, starting on column 1 and extending through the columns
- **Dark current estimate: 7.0685e-4 e^- $pixel^{-1}$ s^{-1}**
  - **Compare with 4e-4 e^- $pixel^{-1}$ s^{-1} given in the EM N2 datasheet or 5e-4 e^- $pixel^{-1}$ s^{-1} given by Harding et al., 2016 for the same temperature**
- **Gain estimate: 1042.0**

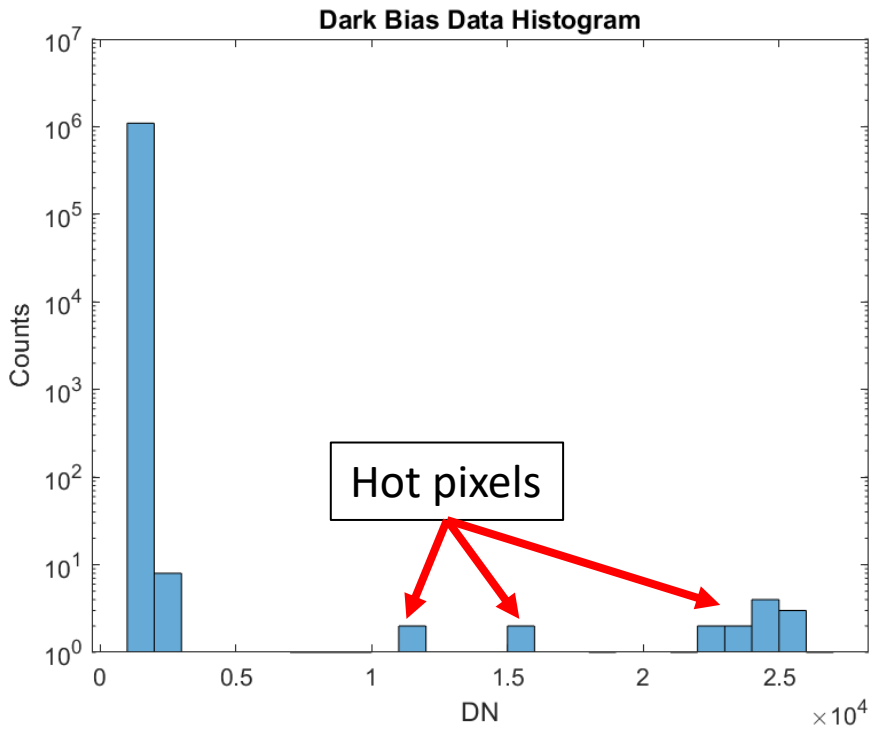

Note: Using the derived dark current rate, expect 7.0685e-2 e^- pix^{-1} fr^{-1} during data collection, well below the 0.2 event $pixel^{-1}$ fr^{-1} limit for minimizing coincidence losses in photon counting, so the assumption of $n = 1$ is appropriate.

Model Validation – Characterization Simulation

- Simulating the previous characterization campaign using the EMCCD Simulator in MATLAB
- Use the test results, EM N2 camera datasheet, and CCD201-20 data sheet to fill-out the simulated detector parameters
- Will be collecting data for:
  - Bias
  - Photon Transfer Curve
  - CIC
  - Dark Current
- Will also be demonstrating quantum yield characterization

Model Parameters

Parameter	Value	Source
Parallel Section Length	50 pixels	*
Parallel Section Width	50 pixels	*
Overscan Elements	16 pixels	+
Standard and Corner Elements	16 pixels	*
Multiplication Elements	50 pixels	*
EM Read Noise	92.798 e^-	^
Parallel Section Full Well Capacity	80000 e^-	+
Serial Section Full Well Capacity	730000 e^-	+
CTE	0.999989	‘
Dark Current Rate	7.0685 e^- $pixel^{-1}$ sec^{-1}	^
CIC Rate	0.0031 e^- $pixel^{-1}$ fr^{-1}	^
Camera Gain Constant	17.7740 e^- DN^{-1}	^
ADC Resolution	16 bits	‘
Vertical Frequency	1 MHz	*
Horizontal Frequency	10 MHz	*

*: Specified
+: CCD201-20 Datasheet
^: From Characterization
‘: From EM N2 Camera Datasheet

Note: A reduced detector size is used in the simulation for the sake of minimizing processing time. This does not impact the behavior of the simulator as compared to a real detector, except for the reduction in the number of multiplication elements, which does alter the shape of the output distribution. This is important for CIC and dark current analysis, as the probability distribution function described in previous slides assumes a large number of multiplying elements. It will be seen that the simulator is still able to well approximate the detector behavior, however this may be a source of deviations from realistic detector operation. See the slide “Output Probability Distribution vs Number of Multiplication Elements” at the end of the slide deck for more information.

Note: For simulating CIC, the rate must be translated from per frame to per transfer. This is accomplished by dividing the CIC rate by the average number of transfers for pixels in the image section.

Bias Simulation

- Comparison of the bias curve generated from camera data and the simulation show the two are similar, though the camera data is not precisely Gaussian in distribution
- Note the lack of fixed pattern noise in the bias frame

Parameter	Value	Source
Bias Level	33397.346 e^-	^
Gain	1	*
Number of Bias Frames	100 Frames	*

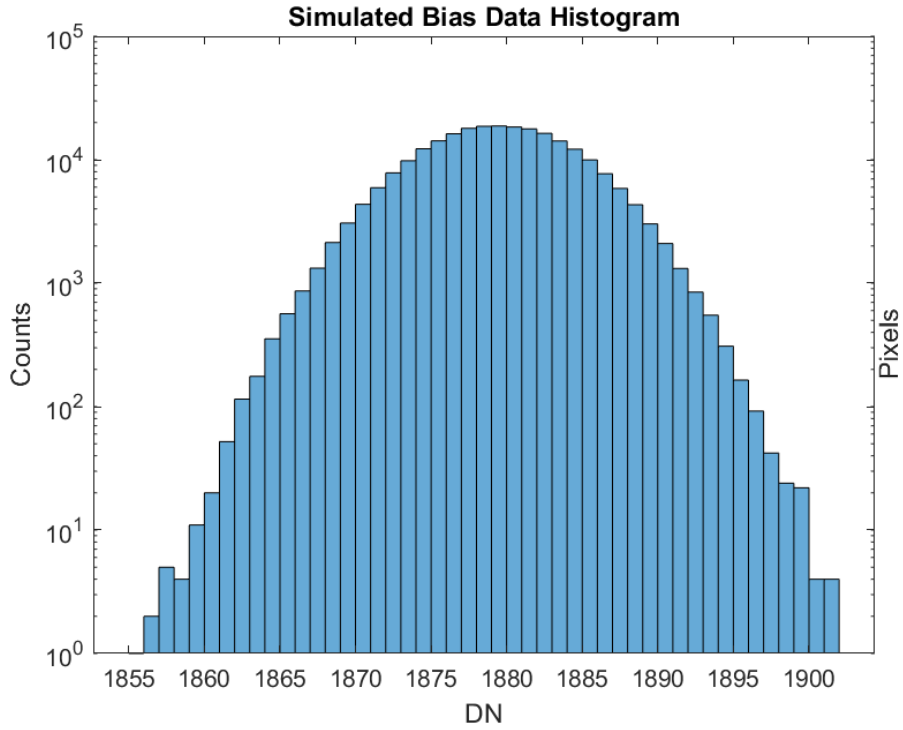

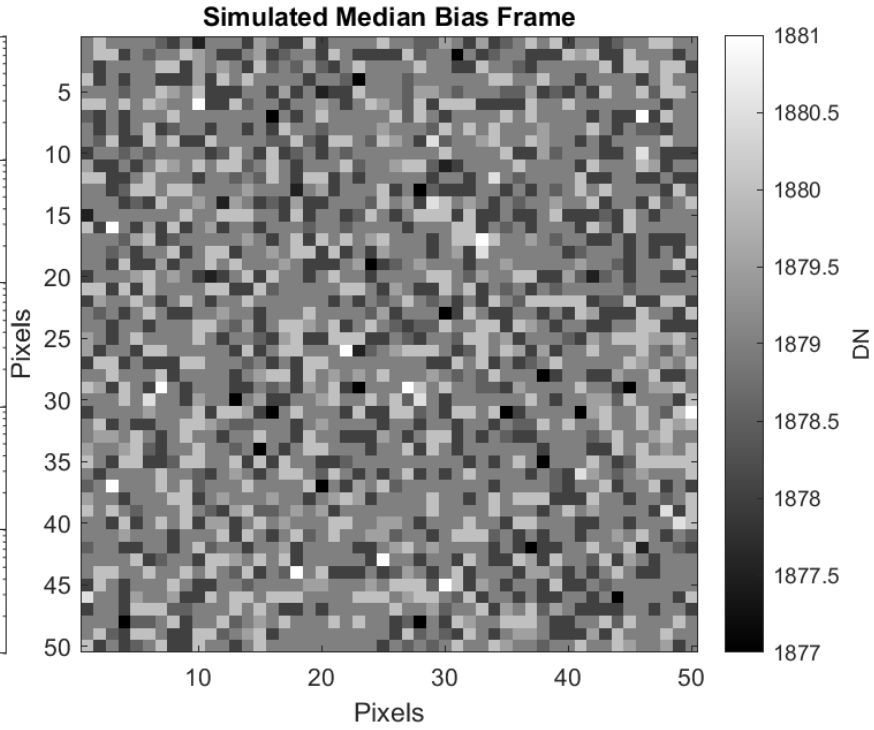

PTC Simulation

- PTC data was taken for exposure times spanning 4 orders of magnitude using 40 sample points, spaced logarithmically
- The simulated light was set to a wavelength of 600 nm with an interacting quantum efficiency of 90% and quantum yield of 1
- Observe that at saturation, the noise level immediately drops to the read noise floor
  - This is because the model does not include non-linearity in charge collection and transfer as a function of the amount of charge in a pixel

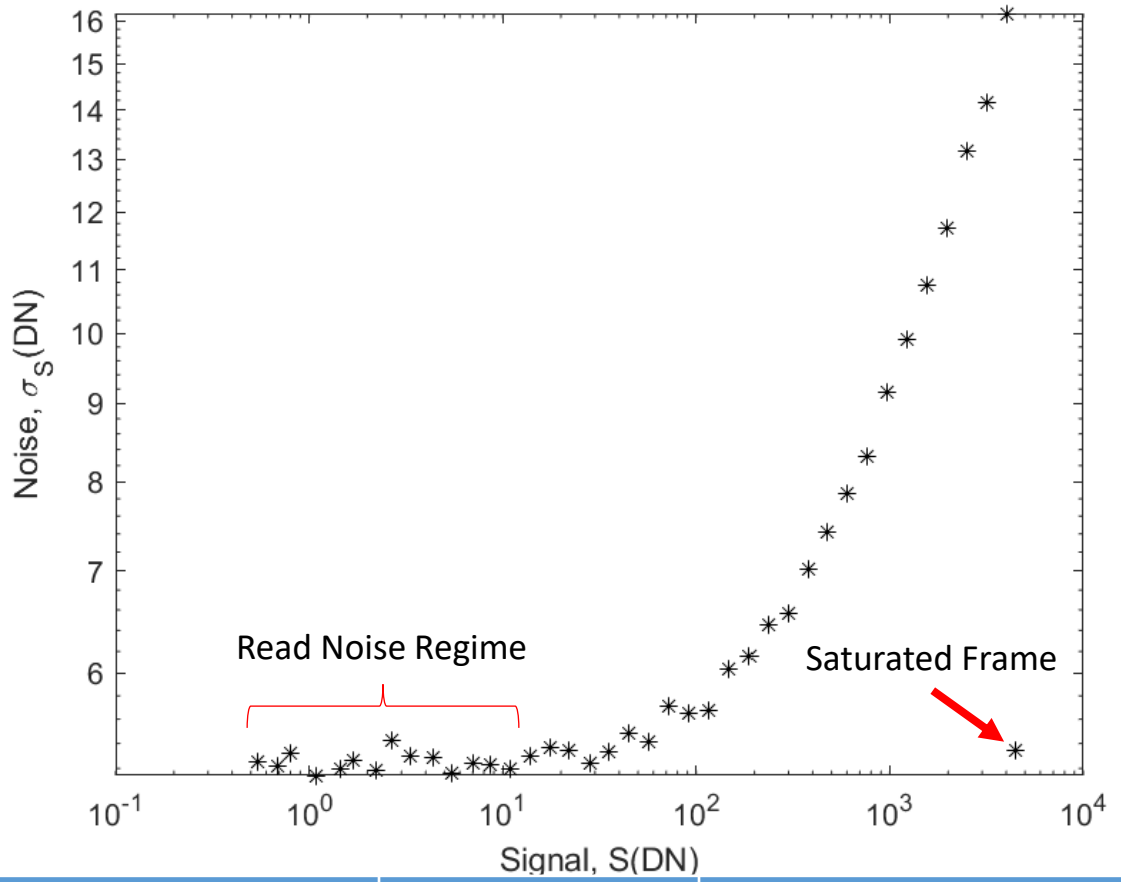

Parameter	Specified	Simulated Measurement
Read Noise	5.2210 DN	5.2449 DN
Camera Gain Constant	17.6665 e^- DN^{-1}	17.6306 e^- DN^-

Quantum Yield Measurements

- For long (> 350 nm) wavelength photons, the photon transfer curve yields the camera gain constant *K*
- For shorter wavelengths, quantum yield is > 1
  - Photon transfer curve now finds the camera gain constant *J*
  - $\eta_i = \frac{K}{J}$
    - η_i is the quantum yield
  - Can find *J* the same way *K* was found previously

Wavelength (nm)	Nominal Quantum Yield	Simulated Measurement	Error (%)
175	1.79	1.99	11.2
0.21	1616.44	1615.82	-0.03

Note: Real measurements of the quantum yield at 0.21 nm will yield a lower value (1420 e^- per interacting photon according to Janesick, 2001) due to the effect of charge collection efficiency. This is not modelled by the (EM)CCD Model, and so approximately the nominal value is recovered.

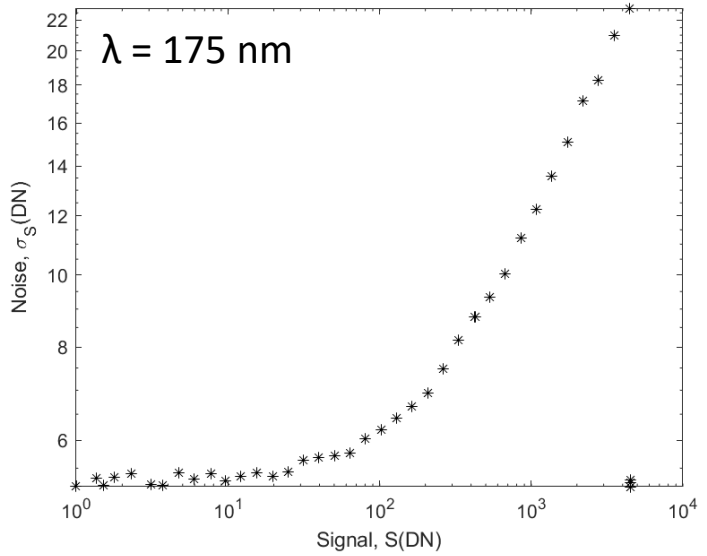

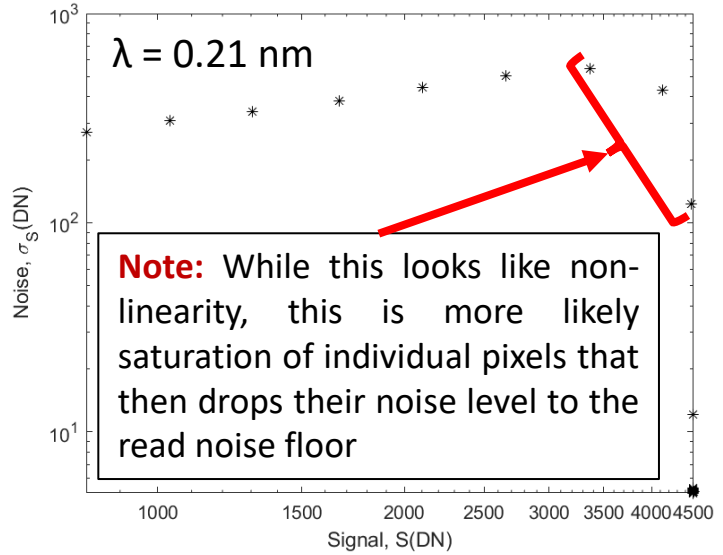

CIC Simulation

- For CIC simulation, the size of the detector parallel section was reduced to 25 x 25 pixels
- In order to simulate the CIC, the measured CIC rate must be converted from per frame, to per transfer
  - Allows the model to simulate CIC on a per pixel basis, in keeping with the working of the rest of the model
  - Divide the per frame CIC rate by the average number of transfers a pixel will undertake in the readout sequence
- **Measured CIC: 0.0031 e^- $pixel^{-1}$ fr^{-1}**
- **Simulated CIC: 0.0027 e^- $pixel^{-1}$ fr^{-1}**
- **% Difference: -12.9%**
- **Retrieved Gain: 1073.2**

Parameter	Value	Source
Bias Level	24030.448 e^-	^
Gain	1000	*
Number of CIC Frames	1000 Frames	*

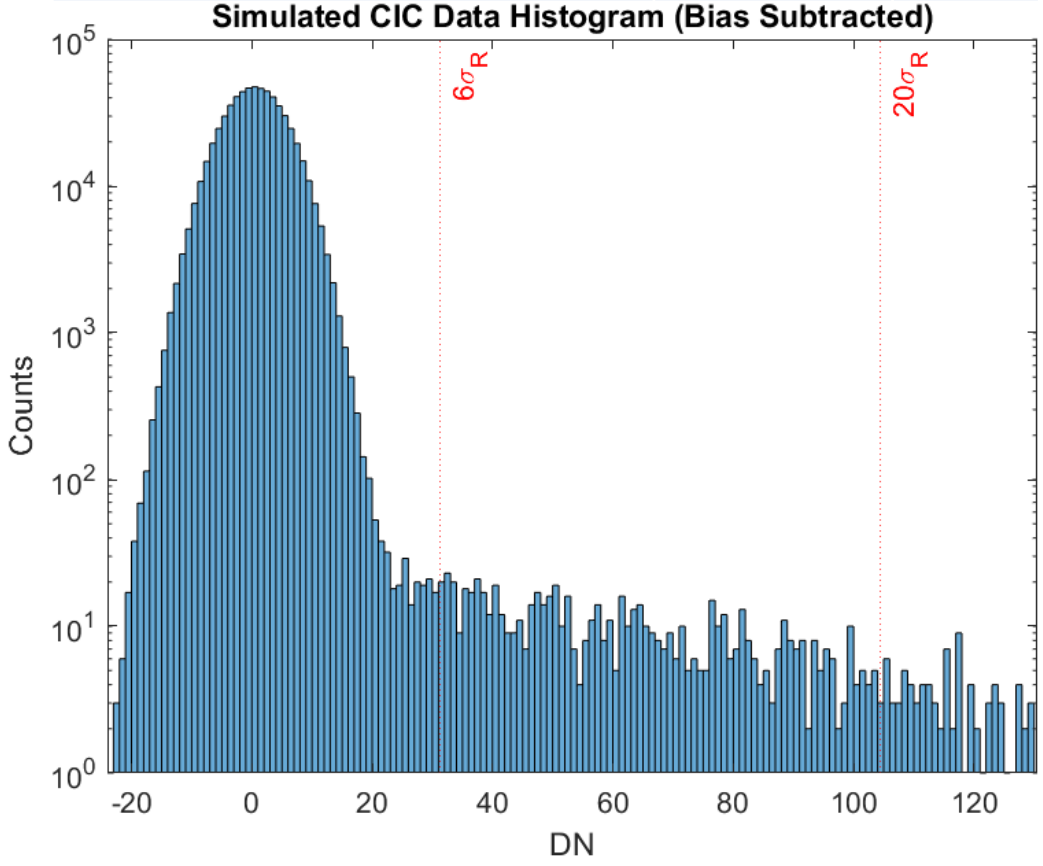

Dark Current Simulation

- Note that the effect of muon impacts on the detector are not included in the simulation
- “Hot” pixels are also not simulated, though the model is capable of doing so if desired
- **Measured Dark Current: 7.0685e-4 e^- $pixel^{-1}$ s^{-1}**
- **Simulated Dark Current: 7.7979e-4 e^- $pixel^{-1}$ s^{-1}**
- **% Difference: 10.3%**
- **Retrieved Gain: 1080.9**

Parameter	Value	Source
Bias Level	23657.194 e^-	^
Gain	1000	*
Number of CIC Frames	144 Frames	*
Integration Time	100 s	*

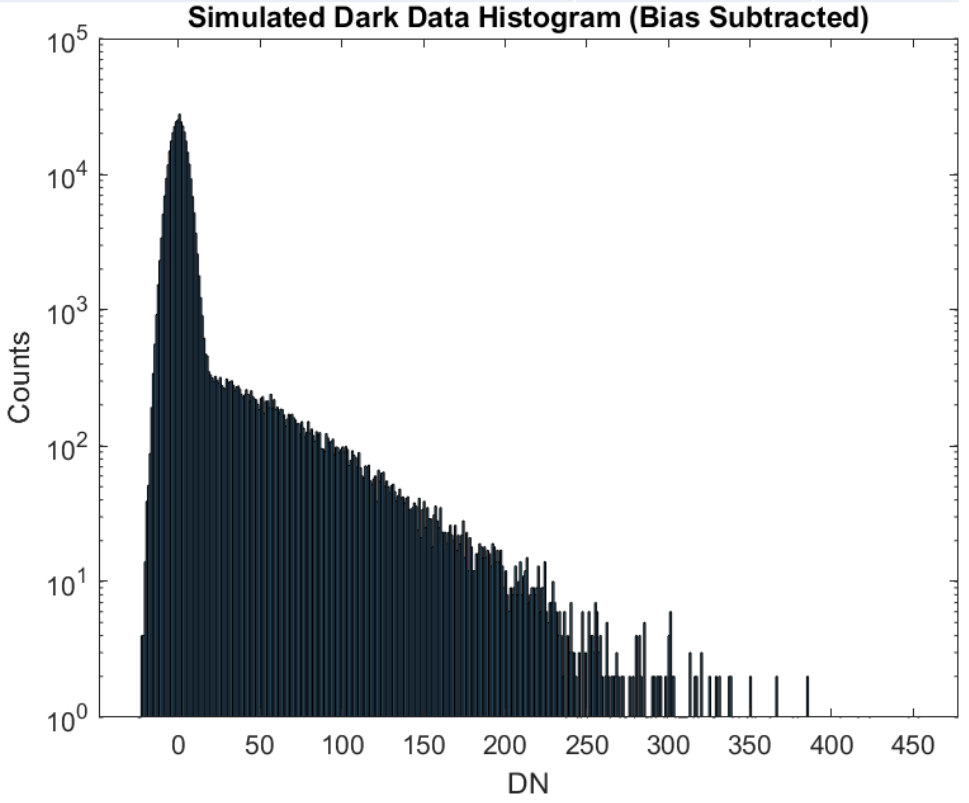

Summary & Future Work

- A model has been developed in MATLAB to simulate each step of the EMCCD readout process
  - Allows for treatment of pixel level noise and charge transfer properties
  - Enables virtual simulation of realistic read-out sequences
    - Image read-out
    - Detector characterization
    - Performance degradation studies
    - Etc.
- Future work will focus on increasing model fidelity, quality-of-life improvements, optimizing performance
  - Treatment of pixel blooming / charge diffusion
  - Extend trap modeling
  - Cosmic ray impacts
  - Ability to incorporate time-dynamic input and pixel properties
- Acknowledgements:
  - Thank you to Dr. Bijan Nemati for reviewing and providing feedback over the course of developing this model.

Code repository is available at:
https://github.com/nj31415/emccd_simulator

References

[1] Bush, N., Hall, D., Holland, A., Burgon, R., Murray, N., Gow, J., Jordan, D., Demers, R., Harding, L. K., Nemati, B., Hoenk, M., Michaels, D., and Peddada, P. "Cryogenic Irradiation of an EMCCD for the WFIRST Coronagraph: Preliminary Performance Analysis." *High Energy, Optical, and Infrared Detectors for Astronomy VII*, Vol. 9915, No. August 2016, 2016, p. 99150A. https://doi.org/10.1117/12.2234628.

[2] Nemati, B., Effinger, R., Demers, R., Harding, L., Morrissey, P., Bush, N., Hall, D., and Skottfelt, J. "The Effect of Radiation-Induced Traps on the WFIRST Coronagraph Detectors." *High Energy, Optical, and Infrared Detectors for Astronomy VII*, Vol. 9915, No. August 2016, 2016, p. 99150M. https://doi.org/10.1117/12.2235278.

[3] Harding, L. K., Demers, R. T., Hoenk, M., Peddada, P., Nemati, B., Cherng, M., Michaels, D., Neat, L. S., Loc, A., Bush, N., Hall, D., Murray, N., Gow, J., Burgon, R., Holland, A., Reinheimer, A., Jorden, P. R., and Jordan, D. "Technology Advancement of the CCD201-20 EMCCD for the WFIRST Coronagraph Instrument: Sensor Characterization and Radiation Damage." *Journal of Astronomical Telescopes, Instruments, and Systems*, Vol. 2, No. 1, 2015, p. 011007. https://doi.org/10.1117/1.jatis.2.1.011007.

[4] Nemati, B. "Photon Counting and Precision Photometry for the Roman Space Telescope Coronagraph." No. December 2020, 2020, p. 271. https://doi.org/10.1117/12.2575983.

[5] Janesick, J. *Scientific Charge-Coupled Devices*. SPIE Press, Bellingham, WA, 2001.

[6] Kuschnerus, P., Rabus, H., Richter, M., Scholze, F., Werner, L., and Ulm, G. "Characterization of Photodiodes as Transfer Detector Standards in the 120 Nm to 600 Nm Spectral Range." *Metrologia*, Vol. 35, No. 4, 1998, pp. 355–362. https://doi.org/10.1088/0026-1394/35/4/23.

[7] McLean, I. *Electronic Imaging in Astronomy - Detectors and Instrumentation*. Praxis Publishing, Chichester, UK, 2008.

[8] Scott, A., Beaton, A., Roy, N., Côté, P., and Hutchings, J. "NUV Performance of E2v Large BICMOS Array for CASTOR." *High Energy, Optical, and Infrared Detectors for Astronomy VII*, Vol. 9915, No. July 2016, 2016, p. 99151T. https://doi.org/10.1117/12.2231750.

[9] Basden, A. G., Haniff, C. A., and Mackay, C. D. "Photon Counting Strategies with Low-Light-Level CCDs." Vol. 991, 2003, pp. 985–991.

Note on Computation Time

- Tracked computation time for a EMCCD readout during the PTC simulations
- Note that the computation time for an exposure increases as more signal builds on a detector
  - The break from exponential growth is due to the model switching to using GPU processing for binomial random number generation
- Computation time increases with the size of the detector, the number of serial elements, and the signal level within the pixels

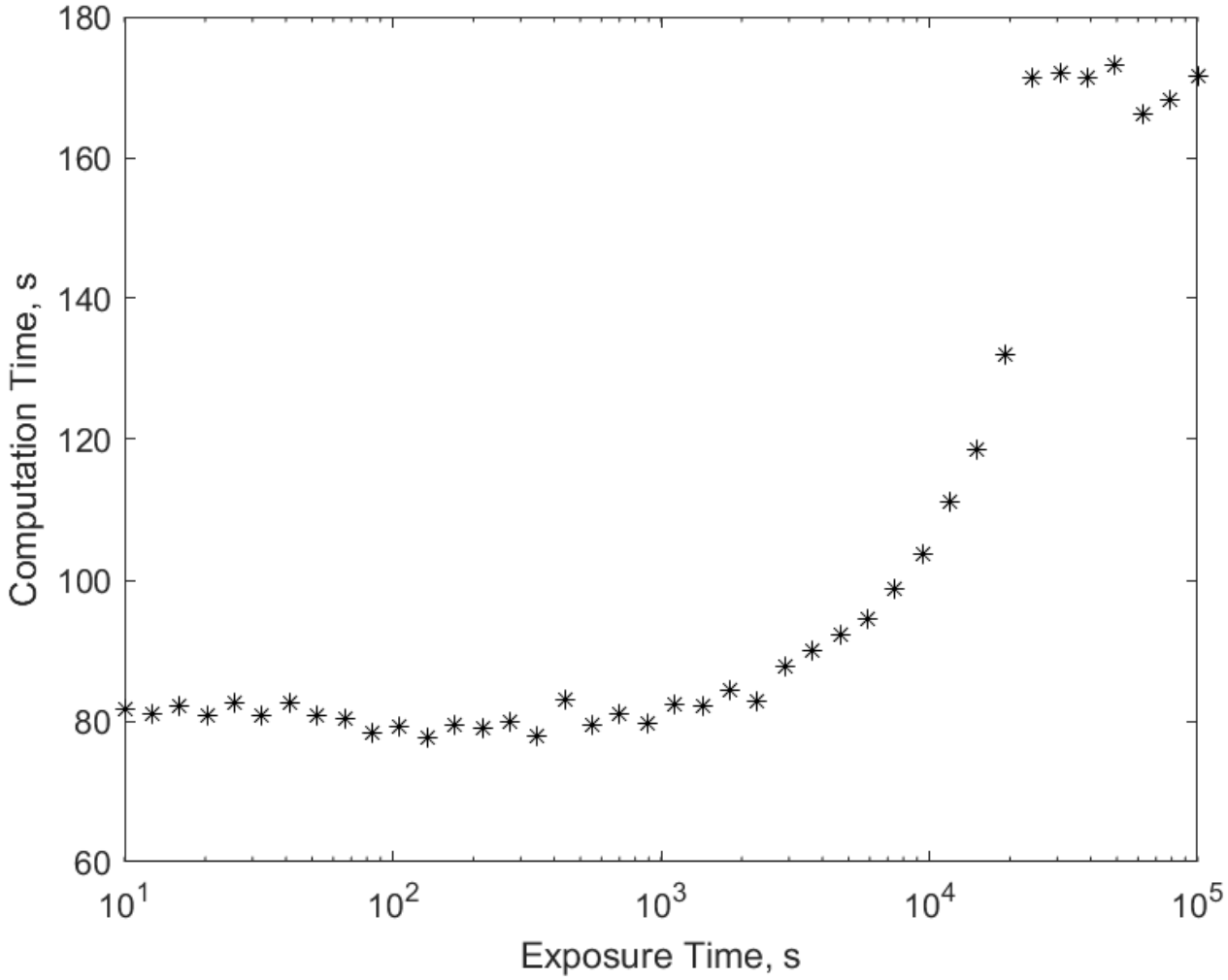

Output Probability Distribution vs Number of Multiplication Elements

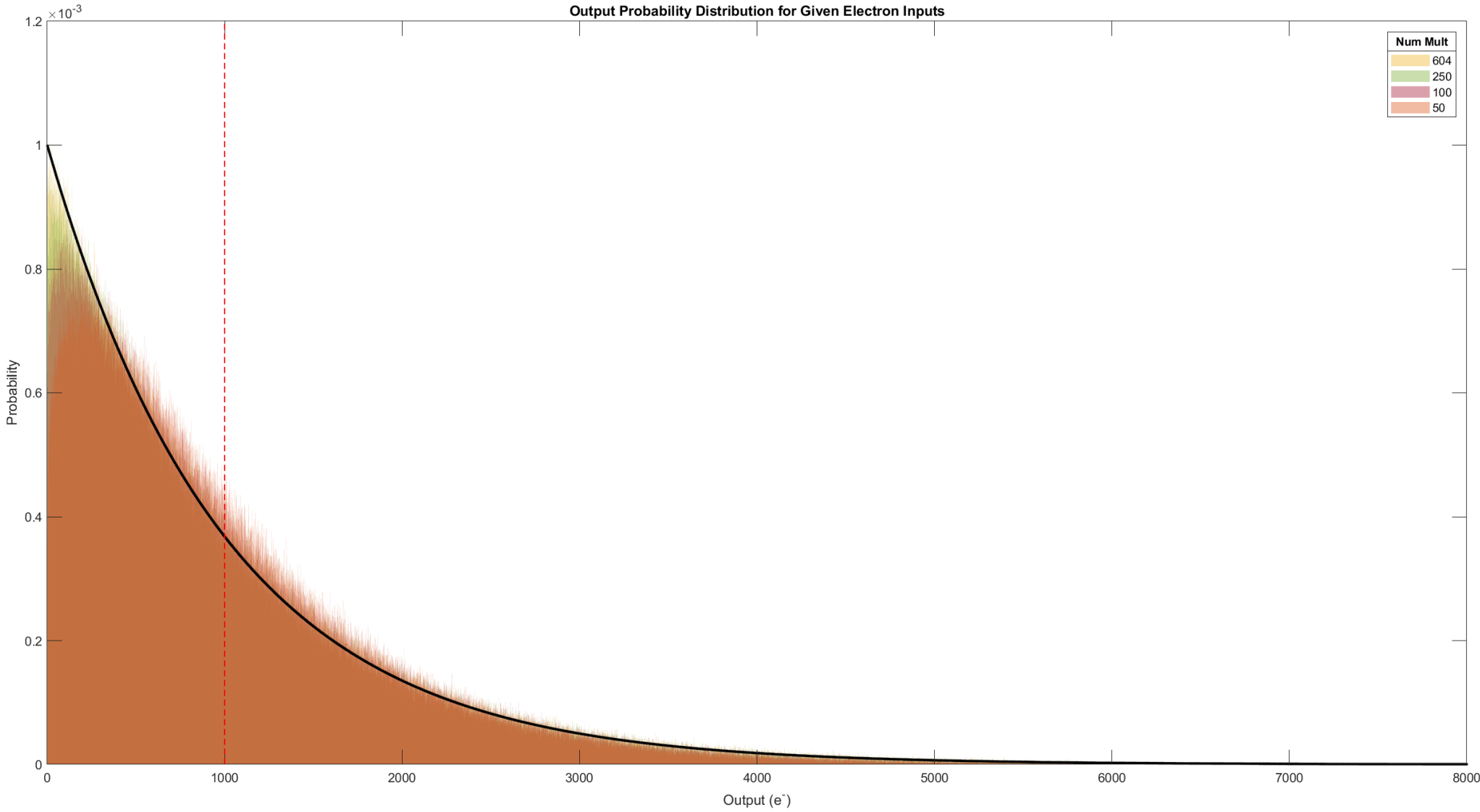

Note: As the number of multiplication elements is decreased, for a constant mean of 1000, the distribution tends to separate from the y-axis, with a higher portion of events being significantly multiplied. The calculated average gain remains constant. This would have the effect of pulling more events out from the read noise in a detector readout